

1972

The kinetics of hydrogen enhanced crack growth in high strength steels

Stephen J. Hudak Jr.
Lehigh University

Follow this and additional works at: <https://preserve.lehigh.edu/etd>

 Part of the [Materials Science and Engineering Commons](#)

Recommended Citation

Hudak, Stephen J. Jr., "The kinetics of hydrogen enhanced crack growth in high strength steels" (1972). *Theses and Dissertations*. 4040.
<https://preserve.lehigh.edu/etd/4040>

This Thesis is brought to you for free and open access by Lehigh Preserve. It has been accepted for inclusion in Theses and Dissertations by an authorized administrator of Lehigh Preserve. For more information, please contact preserve@lehigh.edu.

**THE KINETICS OF HYDROGEN ENHANCED CRACK GROWTH
IN HIGH STRENGTH STEELS**

Stephen J. Hudak, Jr.
Department of Metallurgy and Materials Science
Lehigh University
Bethlehem, Pennsylvania 18015

Abstract

Sustained-load subcritical crack growth kinetics in high purity gaseous hydrogen environments have been examined over the temperature range from -60°C to $+100^{\circ}\text{C}$. The rate limiting velocity was shown to be thermally activated with an activation energy of 3.8 ± 0.8 kcal/mole for the temperature range from -60°C to 23°C . No detectable crack growth was observed from 40°C to 100°C at stress intensity levels up to 50 ksi $\sqrt{\text{in}}$. One-half power pressure dependence was observed only over certain ranges of pressures and temperatures. Substantial deviations from this pressure dependence occurred over other regions depending on these same variables.

THE KINETICS OF HYDROGEN ENHANCED CRACK GROWTH
IN HIGH STRENGTH STEELS

by
Stephen J. Hudak, Jr.

A Thesis

Presented to the Graduate Committee

of Lehigh University

in Candidacy for the Degree of

Master of Science

in

Metallurgy and Materials Science

Lehigh University

1972

This thesis is accepted and approved in partial fulfillment of the requirement for the degree of Master of Science.

September 11, 1972
(date)

Robert W. Wei
Professor in Charge

J. J. Chou
Departmental Advisor

G. P. Conrad
Chairman of Department

ACKNOWLEDGMENT

The author expresses his gratitude to Professor Robert P. Wei for his guidance during the course of this research. His personal interest and patience during the period of graduate study will long be remembered.

Acknowledgment is also extended to Mr. John FitzGerald for his invaluable contribution to the experimental portion of this work.

The author also extends his thanks to Professor Y. T. Chou for serving as Departmental Advisor, to Professor Gary W. Simmons for generously contributing his time to discussion, and to Miss Janet Summers for patiently typing this manuscript.

The author gratefully acknowledges the financial support provided by Lehigh University's Center for Surface and Coatings Research during his first year of study and the American Iron and Steel Institute during the past year of study.

Finally, the author expresses his appreciation to his wife, Jane, for the understanding and encouragement shown during the period of this research.

TABLE OF CONTENTS

Title Page	i
Certificate of Approval	ii
Acknowledgment	iii
Table of Contents	iv
List of Figures	v
Abstract	vi
I. Introduction	1
II. Literature Survey	5
High Pressure Gaseous Hydrogen	5
Low Pressure Gaseous Hydrogen	10
Embrittlement Mechanisms - A Commentary	16
III. Material and Experimental Work	19
Material and Specimen Type	19
Crack Monitoring System	20
Environmental Control System	22
IV. Results and Discussion	24
Crack Growth Behavior	24
Effect of Temperature	25
Effect of Pressure	27
Additional Results	29
V. Conclusions	32
VI. Figures	33
References	49
Vita	53

LIST OF FIGURES

- Figure 1** Schematic of Environment Enhanced Crack Growth Behavior
- Figure 2** Center Cracked Specimen with Potential and Current Leads
- Figure 3** Schematic of Electrical Potential Crack Monitoring System
- Figure 4** Electrical Potential Versus Visual Measurements of Crack Length
- Figure 5** Schematic of Environmental Control System
- Figure 6** Hydrogen Enhanced Crack Growth at Room Temperature
- Figure 7** Hydrogen Enhanced Crack Growth at 2°C
- Figure 8** Hydrogen Enhanced Crack Growth at -20°C for Various Hydrogen Partial Pressures
- Figure 9** Hydrogen Enhanced Crack Growth at -30°C for Various Hydrogen Partial Pressures
- Figure 10** Hydrogen Enhanced Crack Growth at -42°C and -51°C
- Figure 11** Hydrogen Enhanced Crack Growth at -60°C
- Figure 12** Composite of Hydrogen Enhanced Crack Growth Curves from 23°C to -60°C at a Hydrogen Pressure of ~1000 torr
- Figure 13** Effect of Temperature on Stage II Crack Growth for Various Hydrogen Partial Pressures
- Figure 14** Effect of Hydrogen Partial Pressure on Stage II Crack Growth at Various Temperatures
- Figure 15** View of Severely Branched Crack at 1000 torr and -64°C, Side A
- Figure 16** View of Severely Branched Crack at 1000 torr and -64°C, Side B
- Figure 17** Effect of Strength Level on Hydrogen Enhanced Crack Growth in 18Nickel Maraging Steel

ABSTRACT

Sustained-load subcritical crack growth kinetics in high purity gaseous hydrogen environments have been examined over the temperature range from -60°C to $+100^{\circ}\text{C}$. The rate limiting velocity was shown to be thermally activated with an activation energy of 3.8 ± 0.8 kcal/mole for the temperature range from -60°C to 23°C . No detectable crack growth was observed from 40°C to 100°C at stress intensity levels up to 50 ksi $\sqrt{\text{in}}$. One-half power pressure dependence was observed only over certain ranges of pressures and temperatures. Substantial deviations from this pressure dependence occurred over other regions depending on these same variables.

I. INTRODUCTION

Significance of the Problem

The degradation of mechanical properties of steels by hydrogen is perhaps the most infamous of problems in the area of environment sensitive mechanical behavior of materials. This phenomenon, commonly termed hydrogen embrittlement, is of concern over a broad technological range -- production, manufacturing, and service. Common processes, such as steelmaking [1,2], welding [3], electroplating [4-7], pickling [8], and corrosion [9-11], are potentially embrittling since all are capable of liberating detrimental hydrogen under certain conditions. Embrittlement that results from the above processes is generally referred to as "internal hydrogen embrittlement," since the embrittlement process involves hydrogen in solid solution in the lattice. This form of embrittlement is differentiated from "hydrogen environment embrittlement," or gaseous hydrogen embrittlement, whereby steels are embrittled as a result of exposure to gaseous environments of hydrogen. Gaseous hydrogen embrittlement can occur over a wide range of hydrogen pressures, down to tens of torr [13-29]. This broad range of susceptibility poses problems in numerous service situations. The current investigation is directed at this element of the embrittlement phenomenon, namely that of gaseous hydrogen embrittlement.

The widespread occurrences of service failures due to hydrogen embrittlement has provided the impetus for numerous investigations of the problem over the past 50 years. The focus of technology over most of this period was

such that a great majority of these investigations dealt with internal hydrogen embrittlement. In spite of these efforts, a basic understanding of the actual embrittlement mechanism remains elusive. Embrittlement by gaseous hydrogen has become a serious problem more recently, and has received attention through the aerospace programs. The outlook for increased use of hydrogen in systems employing its unique properties requires a solution to the problem of hydrogen environment embrittlement. This solution depends on the achievement of a fundamental understanding of the mechanism for gaseous hydrogen embrittlement.

Scope and Purpose

Various measurements have been used to characterize gaseous hydrogen embrittlement. Decreases in such properties as ductility, ultimate tensile strength, and notched tensile strength relative to the unembrittled condition have frequently been utilized. This type of information has been useful in categorizing materials with respect to their degree of susceptibility, and, therefore, has been helpful in material selection. However, such information is of limited value. Being largely qualitative, it is difficult to derive basic information relative to the nature of the embrittlement process from such data. There also exists a problem of interpretation of these results under embrittling conditions because of the early formation and growth of cracks in the specimens [15, 21].

Since crack growth is an integral part of the hydrogen embrittlement

phenomenon, it seems reasonable to consider this factor in investigating the problem. Furthermore, since crack extension and hydrogen interactions with the metal occur in the highly stressed region of the crack tip, the stress field in the vicinity of the crack tip is most relevant. Consequently, the present investigation has chosen to use the crack tip stress intensity, defined by linear elasticity, to characterize the mechanical crack driving force, since it represents a single parameter characterization of the stress field at the crack tip. The approach taken is to examine the kinetics of crack growth, since hydrogen enhanced crack growth is likely to be related to the kinetics of hydrogen-metal interactions.

Environment enhanced growth rate as a function of stress intensity has exhibited a similar character for a number of environments and is illustrated in Figure 1 [12, 23, 24, 27-29]. Crack growth commences from some apparent threshold stress intensity, K_{th} , which is defined as the level of stress intensity below which no observable crack growth occurs. For low K levels, the rate of crack growth is strongly dependent on K (Stage I). At intermediate K levels, the rate of crack growth becomes relatively independent of K (Stage II). As K approaches K_c , a rapid increase in growth rate (Stage III) occurs, since the onset of unstable fracturing (that is, specimen failure) is approached.

In the present investigation, growth rate data were obtained in Stage I and Stage II; no data were obtained in Stage III, since for the purposes of this study, these rates were of little importance. Attention was primarily focused

on Stage II growth, since its independence of mechanical driving force suggests the operation of a chemical rate limiting process. The purpose of the present investigation was to develop information, in terms of this rate limiting growth, that is necessary for assessing the rate controlling process for hydrogen enhanced crack growth. The activation energy and the pressure dependence for Stage II growth were determined, and will be used in conjunction with companion data on chemical kinetics to assess the mechanism for hydrogen-enhanced crack growth in the future. Observations on the effect of temperature and pressure on the apparent K_{th} were also made.

II. LITERATURE SURVEY

A brief review of some of the important experimental results on gaseous hydrogen embrittlement is given in this section. The intent is to establish a framework for presentation and discussion of the present data. Emphasis is placed, therefore, on those results that are most relevant to the present investigation. A more general review is also presented on the mechanistic theories in an attempt to relate this study to the overall problem of hydrogen embrittlement.

High Pressure Gaseous Hydrogen

Embrittlement by high pressure gaseous hydrogen is not a new problem. Service failures were reported by Bridgman [33] as early as 1924. He encountered repeated failures of Cr-V steel pressure vessels used for compressibility studies of hydrogen gas at 8710 atm (128,000 psi), in spite of the fact that significantly greater pressures could be safely achieved with liquids or gases other than hydrogen. Similar experiences were subsequently reported [34-36], some of which occurred at hydrogen pressures as low as 136 atm (2,000 psi). These failures, in combination with the trend in chemical processing toward higher pressure techniques, provided the initial motivation for investigating the problem of gaseous hydrogen embrittlement.

In attempting to determine which materials could safely be used in the presence of high pressure hydrogen, Dodge and co-workers [13,14] examined nearly 50 metals and alloys. Interestingly, however, mechanical properties were not measured while specimens were exposed to hydrogen. Instead, the

established method for investigating internal hydrogen embrittlement was followed, that is, "charging periods" were employed during which specimens were exposed to high pressure hydrogen prior to testing in air. For such a procedure, however, the only hydrogen available for embrittlement during testing was that which had gone into solution as a result of absorption during the "charging period." The measured embrittlement, being a direct reflection of the hydrogen transport mechanism, was, therefore, not representative of the embrittlement encountered in service failures where gaseous hydrogen is readily available to the plastically deformed regions.

Hofmann and Rauls [15] were the first to recognize the need to characterize embrittlement in the presence of gaseous hydrogen. They measured the ductility and ultimate tensile strength of a low carbon (0.22% C) steel in hydrogen environments that ranged in pressure from 11 atm (162 psi) to 159 atm (2,220 psi). Embrittlement increased with hydrogen pressure; thus identifying pressure as an important variable. It was concurrently observed that the frequency of crack formation increased with increasing hydrogen pressure. Furthermore, these cracks only formed when hydrogen was available during plastic deformation.

The importance of the interaction between hydrogen and deformed material is further demonstrated by results on the effect of pre-exposure to hydrogen. Steinman et al [17] exposed specimens of quenched and tempered 4140 steel (154,000 and 230,000 tensile strength) to hydrogen at 680 atm for periods up to 20 hours prior to testing. The notched tensile strength in hydrogen was

found to be the same for these specimens as for specimens which had not been pre-exposed. Additionally, when tests were conducted in air, subsequent to the same pre-exposure conditions, the low strength steel exhibited no embrittlement while the high strength steel was measurably embrittled. Thus, although embrittlement may result from hydrogen diffused generally within steels, maximum embrittlement occurs when hydrogen gas is present during plastic deformation.

Stress rupture tests of 4140 steel performed in high pressure gaseous hydrogen were found to result in failure very soon after load application or not at all [16]. In addition, failure did not occur under static load (for times up to 8 hours) at stresses significantly below the failure stresses obtained in simple tensile tests under the same environmental conditions. These results are in contrast to those of Troiano and co-workers [37, 38] on hydrogen-charged steels in which delayed failure was observed over a wide stress range and well below the tensile strength of charged specimens after a period of time that depends on stress level. This difference in behavior indicates that gaseous hydrogen embrittlement provides for a rapid transport of hydrogen to the location in the lattice where the actual embrittlement process occurs.

Although various investigations have suggested an influence of temperature on embrittlement [13, 17], there have been few comprehensive investigations on the effect of this variable. Hofmann and Rauls [15] found temperature to have a significant effect on tensile ductility in hydrogen in the temperature range from 90°C (194°F) to 170°C (338°F) at 150 atm (2, 220 psi). Embrittlement in a

cold drawn and in a normalized 0.22% carbon steel exhibited maxima at 0°C and -40°C respectively, with embrittlement decreasing from these values at both ends of the temperature range.

In recent years, Walter et al [21] have measured the susceptibility of a wide range of engineering alloys. Notched ($K_t \approx 9$) and unnotched tensile test results were obtained in 680 atm (10,000 psi) hydrogen, and were compared with results from tests in helium at the same pressure. In agreement with previous results [15], notched tensile strength was found to be a more sensitive measure of embrittlement, since strengths for smooth specimens were unaffected by hydrogen for many of the lesser embrittled materials. For the extremely embrittled high-strength steels, 50 to 88 percent reduction in notch strength, and 62 to 100 percent reduction in ductility were measured. Low-strength steels were found to be embrittled to a lesser degree. A generalization in terms of strength level is difficult, however, since different materials with approximately the same mechanical properties can exhibit great differences in the degree of embrittlement [16]. For a given material, heat-treated to several strength levels though, it is generally true that susceptibility to embrittlement increases with strength level [17].

Variation in strain rate has been shown also to have an effect on gaseous hydrogen embrittlement. Hofmann and Rauls [15] found that the largest decrease of tensile ductility in 0.22% carbon steel, tested in hydrogen at 150 atm (2,220 psi), occurred at the slowest strain rate. Reduction in tensile ductility decreased with increasing strain rate. Embrittlement, however, was

still measurable at strain rates up to 300% per minute. The same qualitative dependence was demonstrated by Vennett and Ansell [18] for notched specimens ($K_t = 4.0$) of 304L stainless steel tested in 680 atm (10,000 psi) hydrogen.

The influence of impurity level on embrittlement was determined by adding small amounts of air, nitrogen, oxygen, and argon to high purity hydrogen environments [15]. As little as 1% by volume of oxygen was found to be sufficient to completely eliminate embrittlement at 150 atm (2,220 psi). With the exception of nitrogen, all other gases had no detectable effect. The slight improvement in ductility accompanying additions of nitrogen was attributed to trace amounts of oxygen present in the nitrogen. The inhibiting effect of oxygen is explained as follows. During plastic deformation of unnotched specimens, virgin material (that is, material which is clean and highly reactive) is exposed on the exterior of specimens. Based on the fact that hydrogen can only enter the lattice in its atomic or perhaps ionic form [39], and that molecular hydrogen dissociates upon chemisorption on iron [40], it is postulated that chemisorption of hydrogen at these highly active surfaces is an essential process to embrittlement. Since oxygen has a high affinity for iron [40], it can be preferentially adsorbed to form an oxide barrier, and thus prevent hydrogen from entering the lattice to cause embrittlement.

The purpose of most of these investigations was to measure the effect of high pressure gaseous hydrogen on mechanical properties in an effort to determine which materials would be safe for applications under similar conditions.

As a result, conditions of temperature and pressure have been very specific, thus, making it difficult to assemble a comprehensive picture of the effects of these variables. In addition, considerable variations in such variables as notch severity [17] and strain rate [15,18] from study to study have provided additional complications in analyzing the entire body of available data. These investigations have, however, served to identify the primary variables, thereby providing a starting point for more fundamental studies.

Low Pressure Gaseous Hydrogen

The substantial embrittlement that can be caused by gaseous hydrogen at low pressures has been recognized only recently. Most of the work in this area of the hydrogen embrittlement problem has been conducted within the framework of linear-elastic fracture mechanics. In general, investigations have been directed at measuring the stress intensity factor, K_{th} , at which observable crack growth commences*, as well as the rate at which these cracks continue to propagate. In addition to supplying important design information, these parameters, through their characterization of the cracking that hydrogen induces, can provide a link between the observed material degradation and the physiochemical processes controlling embrittlement.

Hancock and Johnson [19] were the first to demonstrate the striking degree of embrittlement that can occur at room temperature as a result of 1 atm

* Many other notations have been used in the literature to denote this apparent threshold value of stress intensity, for example, K_{ISCC} , K_{SCC} , K_{It} , or K_i .

(14.7 psi) hydrogen. For the H-11 steel (230,000 psi yield strength) that they investigated, crack growth was observed at a very low stress, corresponding to a K_{th} of 11 ksi $\sqrt{\text{in}}$. In agreement with previously cited observations [15], additions of argon, helium, and nitrogen did not alter the degree of embrittlement. The addition of as little as 0.6% by volume of oxygen, however, was sufficient to completely eliminate observable crack growth. Moreover, cracks could not be restarted until oxygen was removed from the environment. More recently, Sawicki [27] reported that 0.4% by volume of oxygen is capable of eliminating observable crack growth in the same material for temperatures ranging from 28°C to 100°C. A significant increase in K_{th} was also found to occur with the addition of less than 0.1% by volume of oxygen. These observations can be explained in terms of the processes of preferential oxygen adsorption and oxide barrier formation suggested by Hofmann and Rauls [15]. The observed resumption of crack growth when oxygen is removed from the environment indicates that hydrogen is capable of reducing the oxide barrier.

In agreement with previous results on smooth specimens at high pressures, it has been demonstrated [19] that exposure of steel to 1 atm hydrogen prior to stressing has no effect on subsequent crack growth in the same environment. This observation, combined with the above results on oxygen, more clearly identifies one of the components of the previously mentioned metal-hydrogen interaction. Apparently, hydrogen adsorption is an important step in supplying atomic hydrogen to the embrittlement process, and the prerequisite for the occurrence of this step is the availability of a clean, highly reactive

surface. Plastic deformation provides such a surface both on the exterior of smooth specimens and at the crack tip of cracked specimens.

A strain rate dependence similar to that occurring in hydrogen charged steels [41] and high pressure hydrogen environments [15, 18] was observed by Williams and Nelson [22] for hydrogen pressures of less than 1 atm (760 torr). The degree of embrittlement was determined by the stress intensity necessary to achieve crack growth during tensile tests (K_{SCG}). Upon varying the displacement rate over the range from 10^{-4} to 10^{-2} psi, it was found that maximum embrittlement, corresponding to the lowest value of K_{SCG} , occurred at the slowest strain rate. The curve of K_{SCG} as a function of strain rate exhibited sigmoidal behavior and shifted to the right for increased hydrogen pressures. This behavior is consistent with observations of crack growth kinetics. A correspondence between the two types of results will be developed in a later section.

Sustained load crack growth in low pressure hydrogen has also been observed in 18Ni(250) maraging steel by Wei and Landes [23] and in AISI 4340 steel by Landes [24]. These investigators measured crack growth rate as a function of stress intensity at room temperature. Both steels were reported to exhibit a stage of crack growth which was nearly independent of K . Such a rate limited velocity, being independent of the mechanical driving force, is suggestive of the operation of a rate limiting chemical process. This behavior is significant and will be discussed later.

Williams and Nelson [22] have conducted a comprehensive study of the effects of temperature and pressure on the kinetics of hydrogen induced slow

crack growth in AISI 4130 steel. Both of these variables were examined at a constant stress intensity factor of 36 ksi $\sqrt{\text{in}}$. The crack growth behavior in 682 torr of hydrogen over the temperature range from -80°C to 80°C could be separated into three distinct regions. At high temperatures the growth rate increased with decreasing temperature (Region I). In the neighborhood of room temperature the growth rate exhibited a maximum and was nearly independent of temperature (Region II). At low temperatures the growth rate decreased with decreasing temperature (Region III). Expressing this behavior in an Arrhenius plot, the data of Region I and Region III are represented by apparent activation energies of -5.5 kcal/mole and 3.9 kcal/mole, respectively. The dependence of pressure on growth rate was of the form p^n , where n closely assumed values of $3/2$, 1 , and $1/2$ for regions I, II, and III respectively.

This observed temperature dependence deviated considerably from that of bulk diffusion of hydrogen in steel which is reported to have an activation energy of 9.0 ± 0.5 kcal/mole [39,42]. On this basis, Williams and Nelson eliminated bulk diffusion as the rate controlling process, and suggested that some heterogeneous reaction involved in the transport of hydrogen from its molecular form in the gas phase to its atomic form on the crack surface is rate controlling. This reaction was tentatively identified as a thermally activated chemisorption process with a physically adsorbed precursor.

Based on this hypothesis Williams and Nelson [22] developed a quantitative relationship for the observed crack growth kinetics. The starting point of their development was an expression obtained by Porter and Tompkins [43] for

the rate of chemisorption of hydrogen on iron. It was assumed that an independent physical adsorption preceded the rate controlling chemisorption process, and that the fractional coverage of this precursor determined the effective area on which the chemisorption process could operate. Furthermore, the physical adsorption of molecular hydrogen was assumed to be in equilibrium with the gas phase and to follow Langmuir behavior. The expression resulting from this analysis showed agreement with the observed pressure dependency for crack growth. The analysis has, however, been criticized by Oriani [44] for being incomplete. Oriani's own analysis resulted in pressure dependence of p^1 or p^0 for essentially the same assumptions cited above, and $p^{\frac{1}{2}}$ or p^0 for the added assumption that equilibrium existed between the gas phase and the chemisorbed atomic hydrogen. The discrepancies between these analyses appear to result from differences in interpretation caused by the lack of unequivocal information on the specific mechanism of chemisorption. Williams and Nelson also reported good agreement between the observed temperature dependence and model prediction. Sawicki [27] pointed out, however, that there was an inconsistency in arriving at this conclusion. Specifically, in estimating the predicted activation energy, the heat of adsorption for chemisorption was used in the Langmuir expression for physical adsorption. The much lower value for the heat of physical adsorption would have yielded an entirely different activation energy for Region I crack growth than that observed. It must be pointed out, however, that this in no way detracts from the significant experimental contribution toward the establishment of the process or processes controlling

the crack growth kinetics in gaseous environments.

The effect of temperature and pressure on K_{th} has recently been examined by Sawicki [27]. At a hydrogen pressure of 813 torr, K_{th} was found to be essentially independent of temperature for the range from -40°C to 80°C . A slight increase in K_{th} with increasing temperatures was attributed to the enhancement of crack tip blunting at higher temperatures. On the other hand, the variation of K_{th} with hydrogen pressures was found to be significant. Results at 0°C , 26°C , and 70°C all indicated a decrease in K_{th} with increasing hydrogen pressure according to the relationship $K_{th} \propto P^{-0.4}$. These results serve to illustrate the importance of a critical combination of mechanical driving force and hydrogen pressure for the attainment of subcritical crack growth. Similar results have been observed in hydrogen charged steels [37]. In this later case, however, the chemical variable is known to be the hydrogen activity in solution.

Sawicki [27] has also conducted an investigation of the effects of temperature and pressure on crack growth. Growth rates in H-11 steel were determined as a function of K for various temperatures in the range from -27°C to 99°C . Stage II crack growth was observed at intermediate temperatures, however, specimen failure occurred before a rate limiting velocity could be achieved at both temperature extremes. The growth rate process was again found to be thermally activated with Stage II growth exhibiting an activation energy of 2.5 ± 0.5 kcal/mole as compared to that of 3.9 kcal/mole discussed by Williams and Nelson [22] for 4130 steel. The Stage I temperature dependence was found to correspond to an activation energy of -3.4 ± 0.4 kcal/mole at high temperatures

and 2.1 ± 0.4 kcal/mole at low temperatures. These values appeared to be independent of K over the range from 25 to 33 ksi $\sqrt{\text{in}}$. The pressure dependence of growth rate was measured at 27°C, 47°C, and 80°C for a constant K of 29 ksi $\sqrt{\text{in}}$. The growth rate was proportioned to p^1 at the two lowest temperatures and $p^{3/2}$ at the highest temperature. These temperature and pressure dependencies cannot be meaningfully compared with the experimental results of Williams and Nelson [22] since they do not correspond to the same stage of crack growth, and therefore, the overall rate controlling processes differ.

Embrittlement Mechanisms - A Commentary

Several mechanistic theories of hydrogen embrittlement have been proposed on the basis of extensive studies on internal hydrogen embrittlement. One theory proposes that embrittlement is caused by the development of high pressures within internal voids due to the precipitation of molecular hydrogen [11, 50-54]. Degradation of mechanical properties is viewed as the result of expansion of these voids into microcracks by the internal pressure, acting in conjunction with the applied stress. This mechanism is commonly known as the pressure mechanism for hydrogen embrittlement. All of the other theories of embrittlement, whether they are based on surface adsorption [55, 56] or binding energy [37, 38, 57, 58], subscribe to the idea of some intrinsic weakening of the lattice due to the presence of hydrogen.

Operation of the pressure mechanism is feasible, however, only when a solution of high thermodynamic activity of hydrogen can develop in the solid.

This mechanism is undoubtedly significant for hydrogen charged steel, and is supported for example by the observed formation of microcracks in the absence of an externally applied stress [54]. Clearly, however, the pressure mechanism cannot be operative in the embrittlement caused by low pressure hydrogen environments, since no pressure difference can exist across a gas-solid interface. One is therefore forced to conclude either that there is something intrinsically different about embrittlement resulting from gaseous hydrogen environments, or that the pressure mechanism acts in conjunction with a more elemental embrittling mechanism. In other words, the question arises as to whether or not gaseous hydrogen embrittlement and internal hydrogen embrittlement are the same phenomenon.

Attempts to answer this question have been based upon comparisons of the phenomenological observations of these "two types of embrittlement." Some of these observations are compatible, others are not (for example, see references 21 and 22). Resulting conclusions are, therefore, dependent upon which comparisons are interpreted as being most significant. As a result there is considerable disagreement on the answers to the above question. It should be recognized that these observations are largely controlled by the kinetics of hydrogen transport to that part of the lattice where actual embrittlement occurs. In gaseous hydrogen embrittlement the overall transport process includes: transport of molecular hydrogen to a plastically deformed region of the surface where it reacts to form atomic hydrogen, possible surface migration (occurring either before and/or after dissociation) of hydrogen, solution and perhaps stress

enhanced diffusion. In internal hydrogen embrittlement the hydrogen is initially in solution at interstitial sites, or at sinks provided by dislocations, grain boundaries, precipitates and voids. Hydrogen transport, therefore, involves interaction with these lattice features and diffusion under stress gradients. Since transport of hydrogen is vastly different in each of the two cases it is not unusual to observe differences in behavior. This is not to say, however, that the elemental embrittlement processes are different for each case. It is difficult to conceive of damage being incurred on the lattice without hydrogen entry (entry being construed to include hydrogen in the first few atomic layers). Furthermore, once hydrogen has entered the lattice its effects should be independent of its source. Therefore, on the most fundamental level, that is, based upon the elemental mechanism responsible for embrittlement, whatever and wherever that may be, the two types of embrittlement are most likely one and the same phenomenon.

III. MATERIAL AND EXPERIMENTAL WORK

Material and Specimen Type

A 18Ni(250) maraging steel was selected as model material for this investigation. This steel is of the class of maraging types which are capable of developing yield strengths up to 350 ksi primarily as a result of a precipitation reaction in a very low carbon (less than 0.03 w/o) Fe-Ni martensite. The nominal composition of the '250' grade maraging steel is as follows: 18.0% Ni, 7.5% Co, 5.0% Mo, 0.40% Ti, 0.10% Al, and balance Fe. Material used in this study was obtained from a vacuum induction melted heat with low residual impurities as a 4-in.-thick by 12 in. by 18 in. ingot. The ingot was hot rolled straightaway into 0.35-in.-thick plate. The plate was then cut into specimen blanks, heat treated, and finished to 0.18 in. thickness by surface grinding. The following heat treatment was used: (1) solution anneal for 1 hour at 1700°F in a protective atmosphere and air cool, and (2) age for 3 hours at 900°F and air cool. Mechanical properties for this steel in the aged condition are as follows: yield strength = 239.2 ksi, tensile strength = 249.9 ksi, elongation (1 in.) = 10%.

Three-in.-wide by 15-in.-long center-cracked specimens, Figure 2, oriented in the longitudinal (LT) direction were used in this investigation. All specimens contained starter notches introduced by electro-discharge machining. All of the specimens were precracked in fatigue in dehumidified argon. Initial cracks approximately 0.1 in. long were extended from each end of the machined notches. In all cases the maximum load employed in fatigue precracking was

kept below the load to be used in subsequent static tests. This procedure insured that the crack tip plastic zone introduced by precracking was less than 25 percent of that developed during static tests in hydrogen. Thus the interaction of hydrogen with the crack tip stress field was not complicated by prior load history. Both fatigue precracking and static testing were carried out in a 100,000 lb. capacity MTS, closed-loop, electrohydraulic machine. This system was operated in load control and provided an accuracy of better than ± 1 percent.

The stress intensity factor, K , for the center-cracked specimen was computed from Equation 1;

$$K = \frac{P}{BW} \sqrt{\pi a \sec(\pi a/W)} \quad (1)$$

where P = applied load, B = specimen thickness, W = specimen width, and a = half crack length. The secant term is a correction for finite specimen width [45] which closely approximates the series correction obtained by Isida [46].

Crack Monitoring System

An electrical potential method was used for monitoring crack growth, utilizing a continuous recording system. This method is based on an increase in electrical resistance of the specimen with crack growth. A constant current is applied to the specimen, and changes in electrical potential are measured between fixed points above and below the crack, Figure 2. A schematic diagram

of the system is shown in Figure 3. An analytical relationship between the electrical potential, V , and crack length, a , for a center-cracked specimen has been derived by Johnson [48] and was used as an analytical calibration curve. This relationship can be differentiated with respect to time to obtain an expression for crack growth rate, da/dt , in terms of V and dV/dt . Thus, in practice, crack length and crack growth rate data can be computed from recordings of V vs. time.

The electrical potential system has been shown to agree well with other crack length measuring techniques for a number of material-environment systems, provided that crack tunneling is taken into account [49]. (This correction was determined from post fracture examinations to be about 0.01 in. [49]). For the case of high strength steels tested in distilled water and gaseous hydrogen, however, large deviations have been shown to exist [24]. Presumably, these deviations are manifestations of the nature of the intergranular fracture process which allows continued electrical contact (or shorting) over much of the crack surface. The correction developed by Landes [24] to account for this shorting was employed in this investigation. It was assumed that the percentage of crack surface in electrical contact is a function of the linear elastic displacement. Thus, this enables an estimate to be made of the electrically shorted length, which can be applied as a correction to the apparent crack length. The form of this function was empirically chosen. The correction procedure has been verified for several materials under conditions which cause shorting. Figure 4 shows

a comparison of crack length measurements from visual and electrical potential methods [24].

In this work a constant current of 2.5 amperes was employed. For the material used, resolution at room temperature was better than 0.001 in. in half crack length, a . Based on the overall system stability, the lower limit for rate measurement was estimated to be the order of 10^{-7} in./sec

Environmental Control System

Dehumidified, high purity hydrogen was used as the test environment. This environment was supplied through the freely flowing system schematically shown in Figure 5, and maintained around the crack by aluminum chambers clamped to the specimen. Dehumidification was accomplished by passing hydrogen (99.999% pure) through a gas purifier (Matheson Model 460 with Model 461-R cartridge) and through a series of cold traps at -196°C . In a few cases a heated palladium membrane purifier was also incorporated in the system immediately upstream from the test chamber to provide additional purification. Cold traps and a silicone, back-diffusion trap were used on the discharge side to reduce back diffusion of impurities.

A rigorous purging procedure was followed before testing. Initial purging was carried out for at least two hours using ultra high purity argon (99.999% pure). During this initial purge, the components of the gas system upstream from the back-diffusion trap, Figure 4, were outgassed by heating to approximately 100°C . The cold traps were then filled with liquid nitrogen,

and the specimen and environment chamber assembly was again heated to 100°C while maintaining argon flow. The system was then evacuated with a mechanical pump and back-filling with hydrogen (99.999% purity). Hydrogen was allowed to flow through the system for about 15 minutes prior to the start of the test. With this procedure the impurity level of the hydrogen environment is estimated to be well below 30 ppm. A slight positive pressure of about 5 psig (\sim 1000 torr) was maintained throughout the experiment. To obtain various partial pressures of hydrogen, hydrogen-helium gas mixtures were used in the above system.

For tests conducted above room temperature, resistance heating tapes were used to heat the specimen. In order to reduce thermal fluctuations, the specimen was wrapped in glass wool which in turn was encased in aluminum foil. Low temperatures were achieved by flowing chilled dry nitrogen through an insulated enclosure around the specimen and hydrogen environment chamber. Temperature was monitored by means of iron-constantan thermocouples spot welded to the specimen at positions both inside and outside of the hydrogen chamber. Temperature stability of better than $\pm 1^\circ\text{C}$ was maintained throughout each test.

IV. RESULTS AND DISCUSSION

The sub-critical crack growth kinetics of 18Ni(250) maraging steel, in dehumidified gaseous hydrogen, were investigated. The growth rate was examined as a function of stress intensity under a slightly positive hydrogen pressure of about 5 psig ($\sim 1,000$ torr) over a range of temperatures from -60°C to 100°C . The effect of hydrogen pressure on crack growth at various temperatures within this range was also determined. Hydrogen partial pressures of 430, 210, and 86 torr were used, and were obtained by employing hydrogen-helium mixtures containing, respectively, 42.0, 20.9, and 8.5 percent hydrogen.

Crack Growth Behavior

The hydrogen enhanced growth rate exhibited the same general dependence on stress intensity as that reported for other high strength steels [24, 27]. As illustrated for example, in Figures 6 and 7, two clearly distinguishable regions of growth were observed, namely, Stage I where the rate is strongly dependent on K , and Stage II, where the rate is nearly independent of K . Stage III growth, in which the rate once again increases rapidly as K approaches K_c , is expected to follow; however, this stage was not observed since tests were terminated before total specimen failure. The character of these curves is a consequence of the fact that the driving force for subcritical crack growth contains a chemical component as well as a mechanical component. The growth rate for any point on the curve must, therefore, be controlled by either the rate at which mechanical energy is supplied to the moving crack, or the rate at

which hydrogen is supplied to that portion of the lattice where embrittlement occurs, or by a combination of these rates. For Stage I growth, the strong dependence on K indicates that the rate of delivery of mechanical energy is important so that kinetic control must lie either entirely or partially in this component. On the other hand, the fact that Stage II growth is independent of mechanical driving force indicates that control lies in some chemical process that supplies hydrogen to the crack tip. In other words, the rate limiting velocity arises from the inability of the "transport mechanism" to maintain some critical concentration of hydrogen at growth rates above this level. It is, therefore, appropriate to focus attention on the crack growth kinetics in Stage II in attempting to relate hydrogen enhanced crack growth to an underlying physiochemical process, since these rates will not be complicated by the mechanical component.

Effect of Temperature

The effect of temperature on the K versus growth rate curves is shown in Figures 6 and 11 for several hydrogen partial pressures. The solid lines drawn through the Stage II data (Figures 6 through 10) represent the average values of the rate limiting velocities. The dashed line in Figure 11 represents an adjusted value of the rate limiting velocity to compensate for the anomalous behavior observed at this temperature. Clearly an increase in K should not be accompanied by a decrease in crack growth rate as appears to occur in specimen 26. Crack branching could cause such an effect; however, it was not

observed to be a problem in this specimen. This behavior was attributed to the presence of a temperature gradient in the specimen. Since the specimen edges (in direct contact with the chilled nitrogen gas stream) would be expected to be slightly colder than the specimen center (shielded by the aluminum chambers), the crack growth rate would be expected to decrease with crack prolongation. This is in qualitative agreement with the observed behavior. A general examination of the growth rate curves also supports this view since a drop off of the plateau rates seems to increase as temperature decreases.

The most comprehensive characterization of the temperature dependence was carried out in hydrogen at $\sim 1,000$ torr. The effect of temperature at this pressure is more clearly represented in the composite curves in Figure 12. It is seen that the effect of temperature on K_{th} is at most very slight. This is in agreement with Sawicki's results on H-11 steel [27]. Representation of the Stage II growth rates in the form of an Arrhenius plot (Figure 13) indicates that Stage II growth is thermally activated with an apparent activation energy of 3.8 ± 0.8 kcal/mole. The scatter bands represent two standard deviations on either side of the mean, or the 95% confidence interval. Data points with downward arrows indicate tests in which no detectable crack growth was observed at K levels up to 50 ksi $\sqrt{\text{in}}$; that is, with rates less than 10^{-7} in/sec. Tests at 50°C and 80°C showed that no detectable crack growth occurred for K levels up to 72 and 84 ksi $\sqrt{\text{in}}$, respectively, at these temperatures. The temperature dependence for Stage II growth at low temperatures (Region III) is quite similar to the activation energy of 3.9 kcal/mole reported by Williams

and Nelson [22] for AISI 4130 steel. In the present study, however, the above room temperature (at 1,000 torr) behavior drops off much more rapidly.

Limited data on the temperature dependence of Stage II growth at lower pressures (Figure 11) appear to exhibit the same activation energy as data at 1,000 torr. Note, however, that the maximum position, corresponding to maximum embrittlement, tends to shift to lower temperatures with decreasing hydrogen partial pressure. Further consideration of these observed shifts leads to some interesting possibilities. It is likely that the shift in the peak position of the temperature behavior curve is a general behavior. If this is so, the Regions I, II, and III, as presently defined, would not be separated by isothermal lines but rather by lines inclined at some angle, whose magnitude would depend upon the amount of shift with pressure. More importantly, however, this shift would cause a variety of pressure dependencies to be observed, depending upon the choice of temperatures at which measurements are carried out. Further discussion of this effect will be made in the following section.

Effect of Pressure

The effect of hydrogen pressure on crack growth kinetics is illustrated in Figures 8 and 9. From the data in Stage I it is difficult to formulate a definitive statement about the effect of hydrogen pressure on K_{th} . The only crack growth curve in which K_{th} appears significantly altered is the one at -30°C and 86 torr (Figure 9). Results in other environments have identified problems associated with extrapolation of Stage I data due to the recently recognized

phenomenon of transient growth [59, 60]. In view of this fact, it is perhaps best to say nothing more about the effect of pressure on K_{th} until such effects can be properly established by constant K tests.

The effect of hydrogen partial pressure on Stage II crack growth is summarized in Figure 14. The solid lines superimposed on the data represent slopes of $1/2$. The growth rates are, therefore, proportional to $p^{1/2}$ over certain ranges of pressures depending upon temperature. However, substantial deviations from a $p^{1/2}$ dependency are indicated by the dashed lines. Once again the data points with downward arrows indicate no observable growth.

Previous studies have determined the temperature dependence for a certain pressure in the neighborhood of 1 atm (760 torr). The temperature dependence was used to identify three regions of crack growth behavior. The effect of pressure was subsequently measured at one selected temperature within each region. This pressure dependence was assumed to be characteristic of the region. Because of the shift of the da/dt vs. $(1/T)$ curves, however, a variety of measured pressure dependencies is possible. For example, referring once again to the isobars of Figure 13, if one chooses the temperature of -10°C to measure the pressure dependence, this isotherm will intersect the 1,000 torr isobar in Region III, the 430 torr isobar in Region II and the 210 torr isobar somewhere in Region I. The intersections corresponding to crack growth rate determinations at the three different pressures will clearly result in a pressure dependence different from that measured at -40°C whose isotherm intersects all the isobars in Region III.

An interesting relationship can be inferred by comparing the crack growth rate versus K curves for different pressure with the displacement rate versus K_{SCG} curves that Williams and Nelson obtained for various pressures. Applying a constant cross head displacement rate is equivalent to demanding a specific crack growth rate for a given crack length and specimen geometry. Considering this correspondence between growth rate and displacement rate, these curves are in fact the same in the absence of transient effects.

The measured effect of pressure on the crack growth rate versus K curve for 18Ni(250) maraging steel indicates a complicated pressure dependence. As shown in Figure 14, there is considerable variation in the expression $da/dt \propto p^n$ which is a strong function of temperature. At the present time no simple models based on the transport kinetics of hydrogen appear to explain this observation. The determination of the rate limiting process for crack growth in Stage II must await the comparison of experimental results on the kinetics of the physiochemical processes involved.

Additional Results

Several specimens of 18Ni(300) maraging steel were also tested in dehumidified hydrogen at room temperature. The purpose of testing this higher strength maraging steel was to provide a comparison with the crack growth behavior in the "250" grade. As anticipated, the embrittlement was found to be more severe for the higher strength material. This increased degree of embrittlement is characterized (Figure 17) by a lowering in K_{th} , the apparent

threshold stress intensity, as well as a factor of three increase in the Stage II growth rate. Increased sensitivity to embrittlement with increasing strength level is also found to occur in steels as a result of internal hydrogen embrittlement [7]. In either case, it is not clear whether this effect arises from a difference in resistance to hydrogen transport or a difference in resistance to the actual process by which hydrogen incurs damage to the lattice. With respect to gaseous hydrogen embrittlement, however, this effect serves to add microstructure to the list of variables that can be used to relate crack growth to possible physiochemical rate controlling processes.

Several experimental complications were experienced. The most troublesome was the fact that occasionally the crack would grow from only one side of the center-cracked specimen. No usable data could be obtained from such a test since the potential system could not monitor the crack for this non-symmetric condition. Additionally, for such a test, a value of K cannot be computed. Cracks were also observed to branch near the ends of a few tests; no useful data could be obtained when this situation occurred either. Both the severity and frequency of crack branching increased with decreasing temperature. Figures 15 and 16 show side "A" and side "B" of one of the severely branched cracks in a center-cracked specimen. The most interesting observation is obtained by comparing the right side of Figure 15 with the left side of Figure 16 and vice versa. The differences in the branched cracks at the surface indicate that the through-the-thickness crack front is complicated. This is in agreement with the intergranular nature of fracture observed by electron

microfractography [23] for the 18Ni(250) maraging steel used in this study. Fracture appears to occur along the prior austenite grain boundaries. This is in agreement with the observation of hydrogen emanation from the austenite islands by Toy and Phillips [61] and is consistent with the occurrence of intergranular fracture in hydrogen induced crack growth in other high-strength steels [22, 27].

V. CONCLUSIONS

The following conclusions can be made on the basis of the experimental results on the 18Ni(250) maraging steel.

1. In the temperature range from -60°C to 23°C , Stage II crack growth is thermally activated and is characterized by an activation energy of 3.8 ± 0.8 kcal/mole. This activation energy is in excellent agreement with that reported by Williams and Nelson for an AISI 4130 steel.
2. No observable crack growth occurred in this material in the temperature range from 40°C to 100°C at stress intensity levels up to 50 ksi $\sqrt{\text{in}}$.
3. At the lower temperatures used in this investigation, the crack growth rate was dependent on hydrogen pressure according to $p^{\frac{1}{2}}$. Significant deviations from the one-half power dependence were observed, however, at low pressures and high temperatures.
4. The pressure dependence for crack growth appears to be much more complicated than that reported previously. Models that have been proposed fail to account for the observed behavior from this study.
5. The strong interplay between temperature and pressure effects suggests that care must be taken in the interpretation of results in arriving at a mechanism for hydrogen enhanced crack growth. Definitive conclusion on the rate limiting process for Stage II crack growth will have to await results from the companion study on the chemical kinetics for this steel.

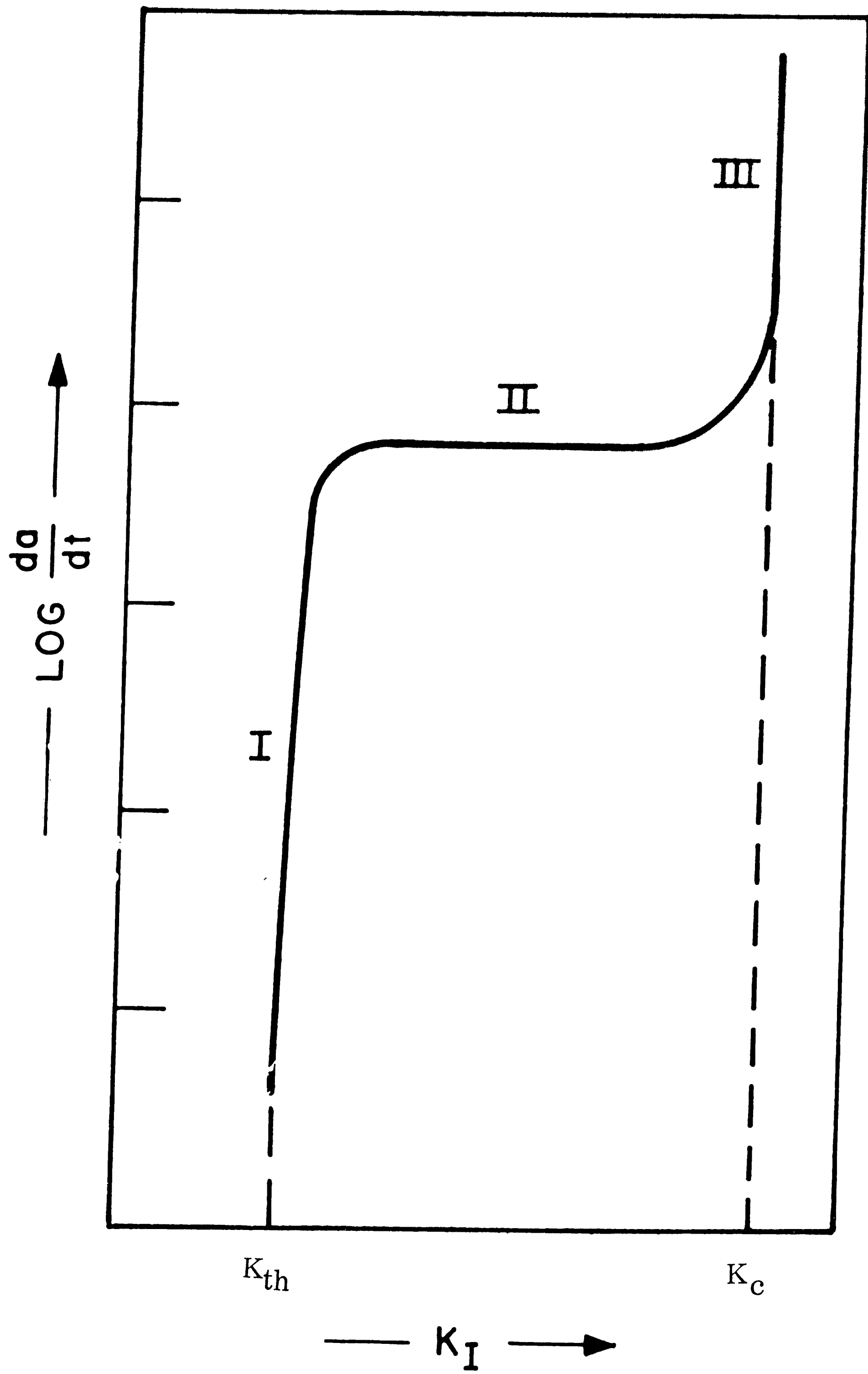


Figure 1: Schematic of Environment Enhanced Crack Growth Behavior

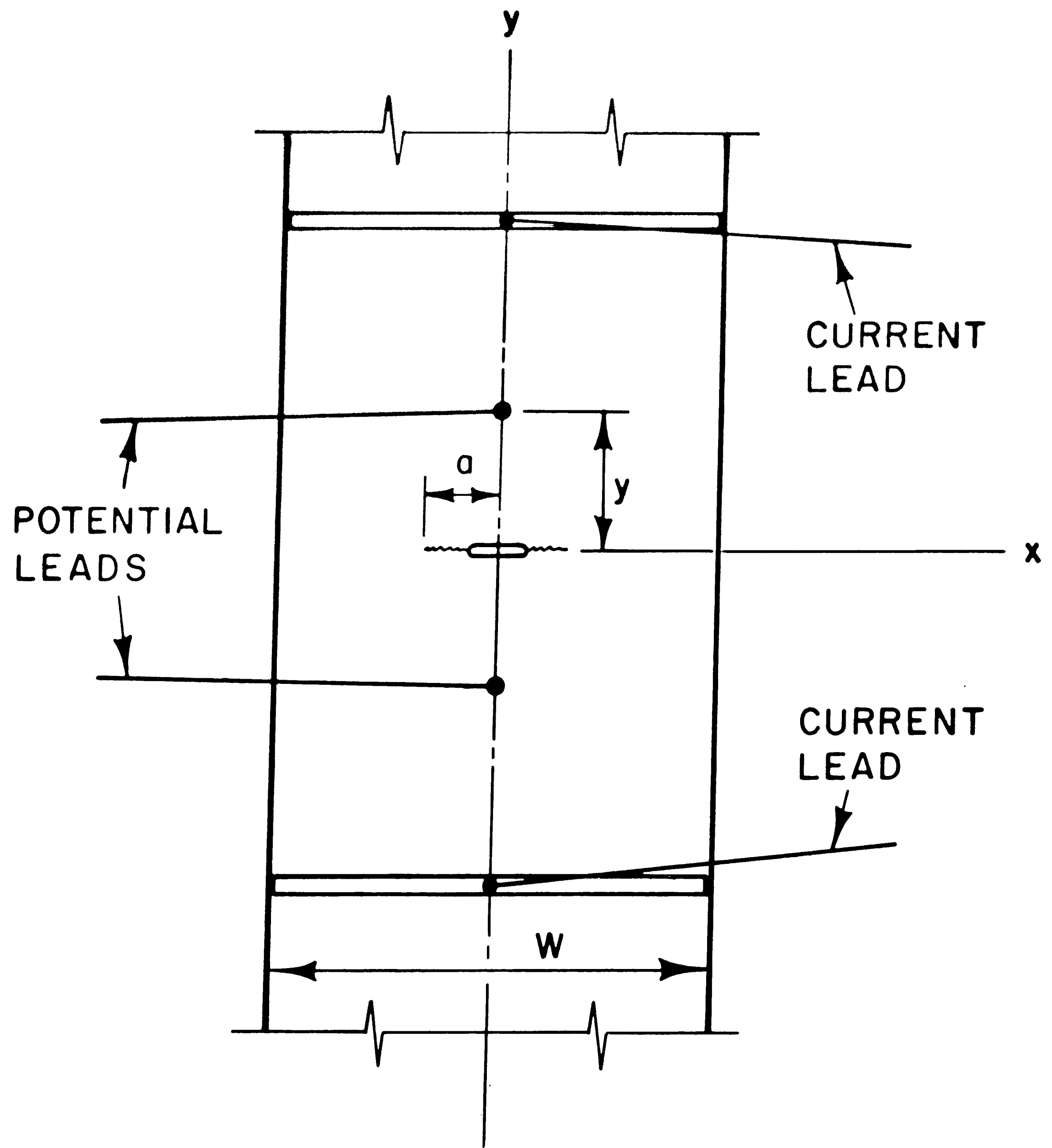


Figure 2: Center Cracked Specimen with Potential and Current Leads

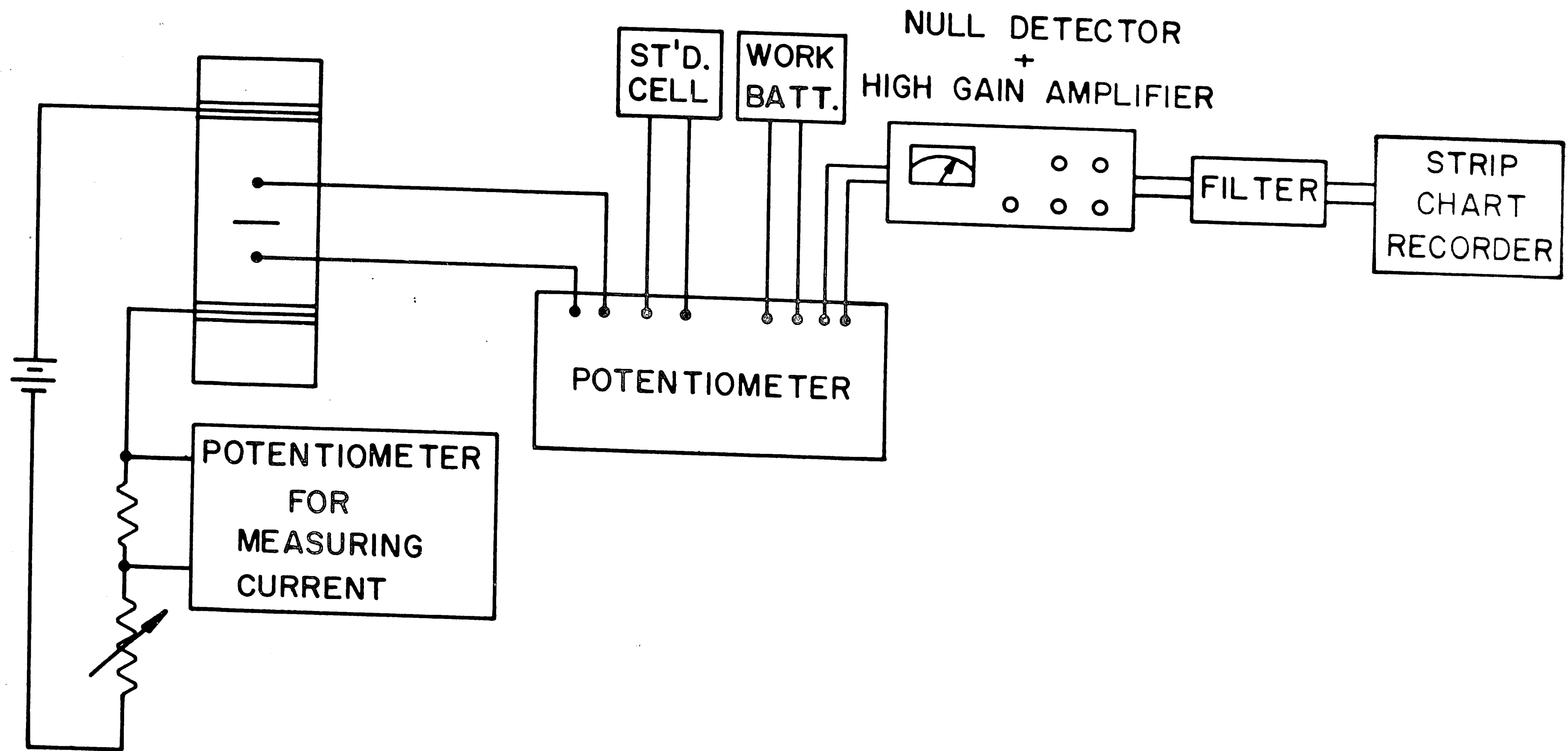


Figure 3: Schematic of Electrical Potential Crack Monitoring System

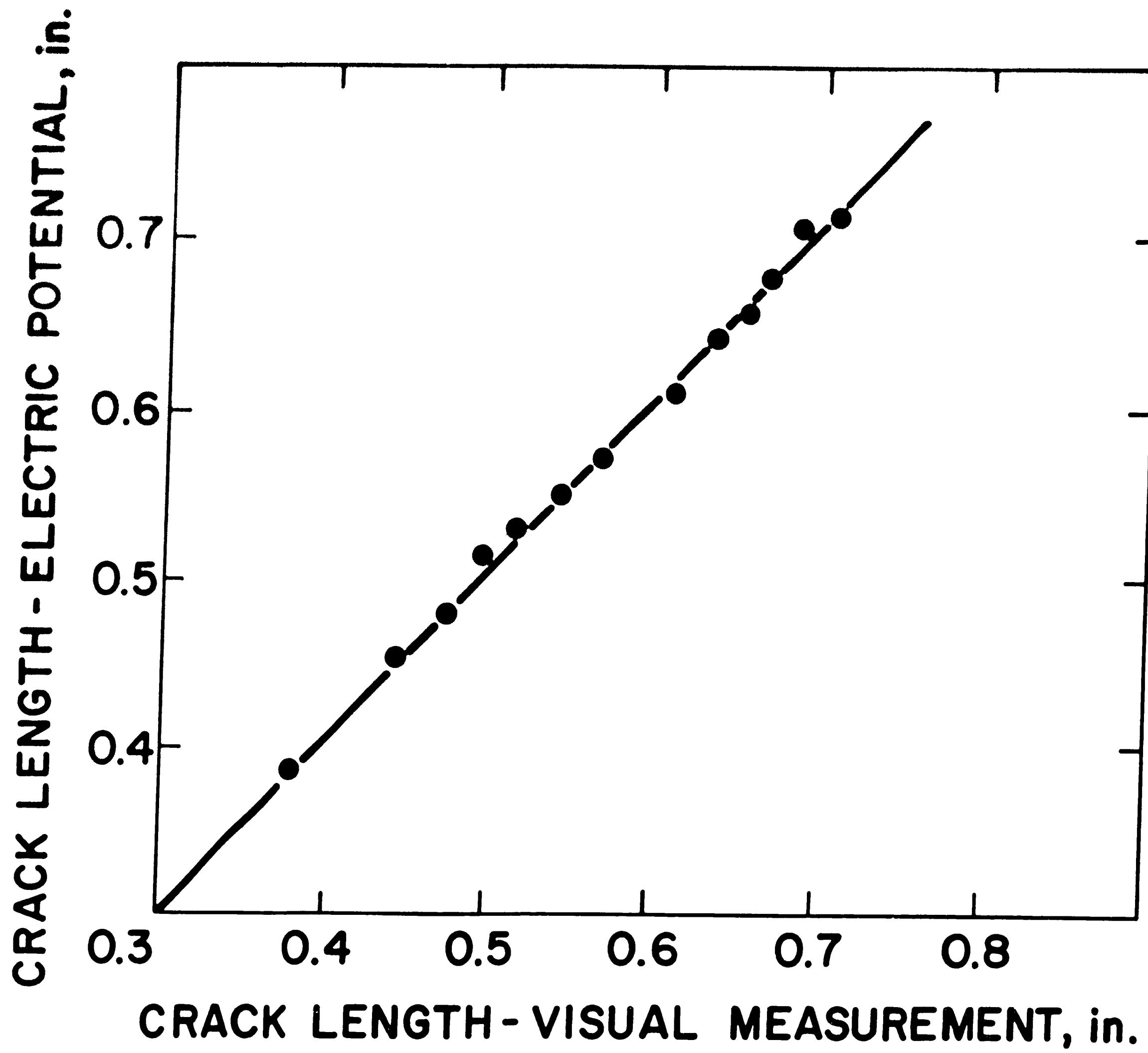


Figure 4: Electrical Potential Versus Visual Measurements of Crack Length

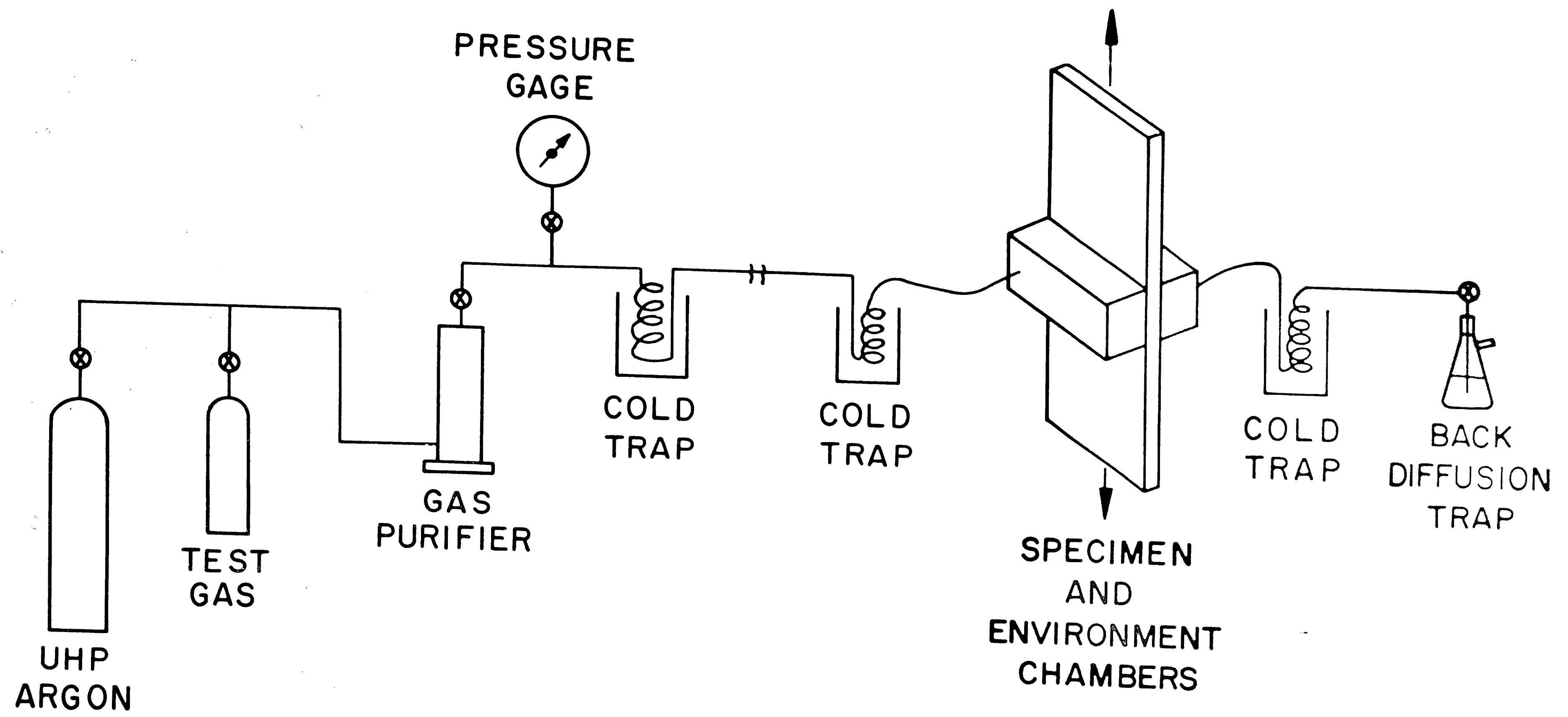


Figure 5: Schematic of Environmental Control System

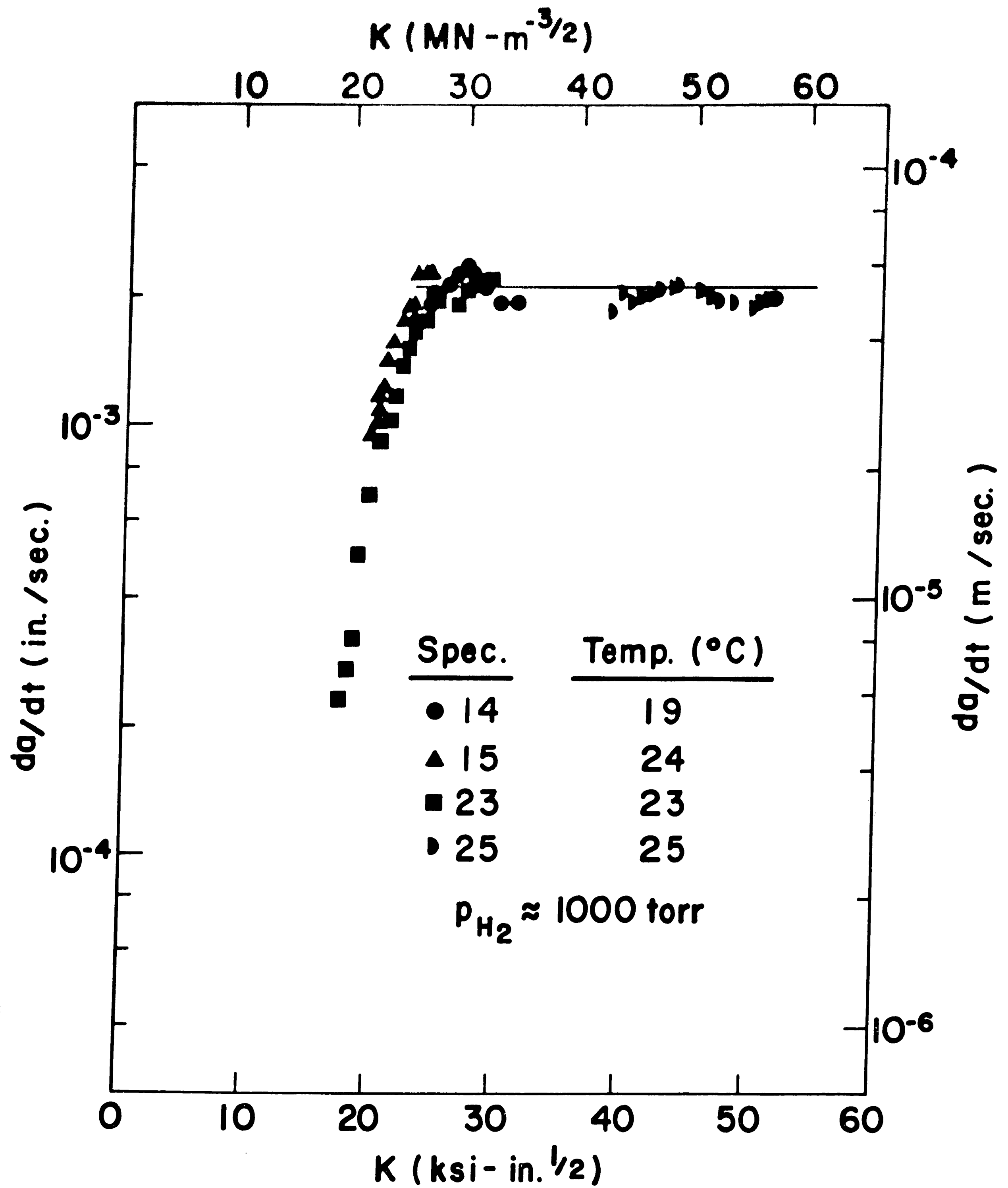


Figure 6: Hydrogen Enhanced Crack Growth at Room Temperature

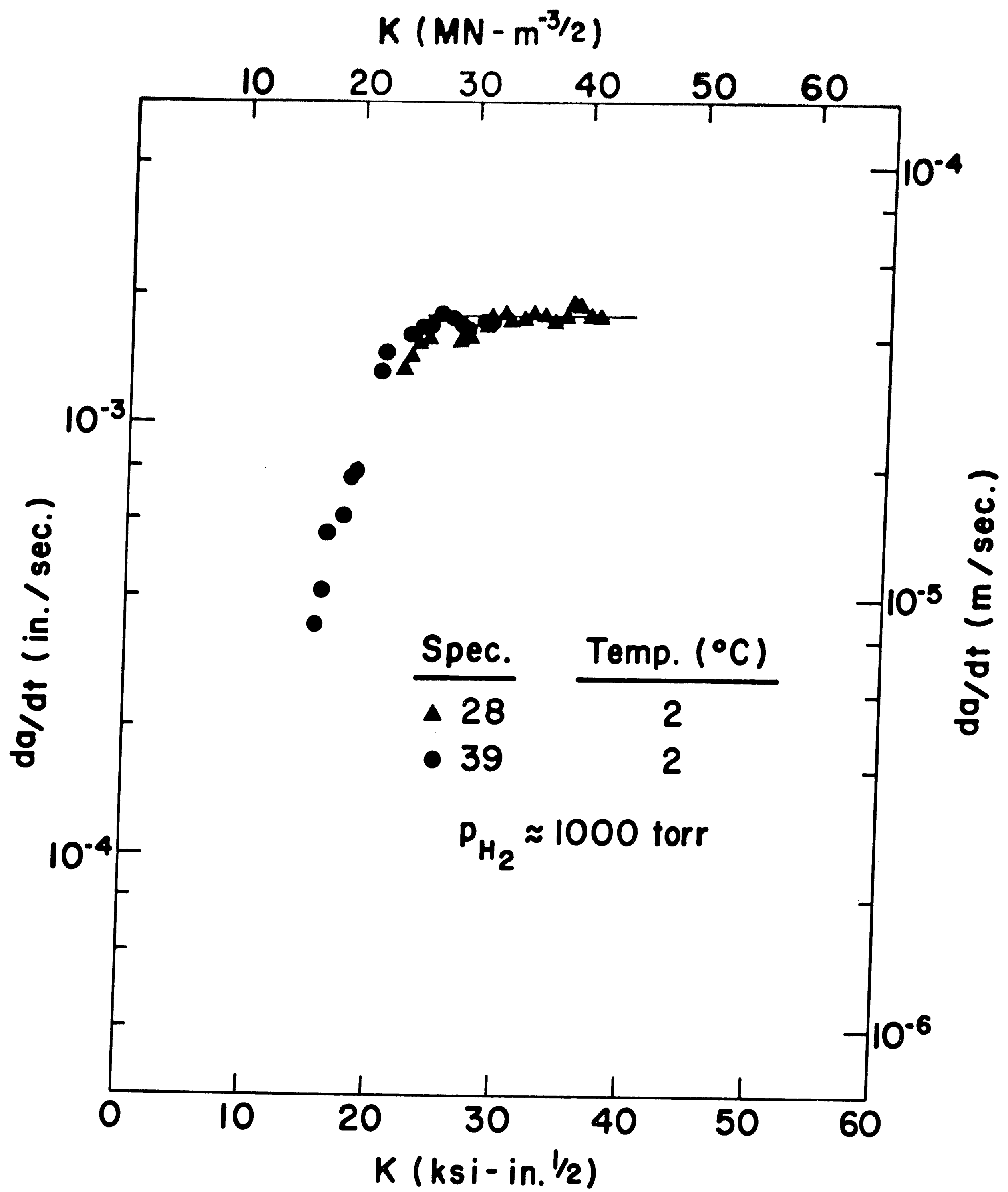


Figure 7: Hydrogen Enhanced Crack Growth at 2°C

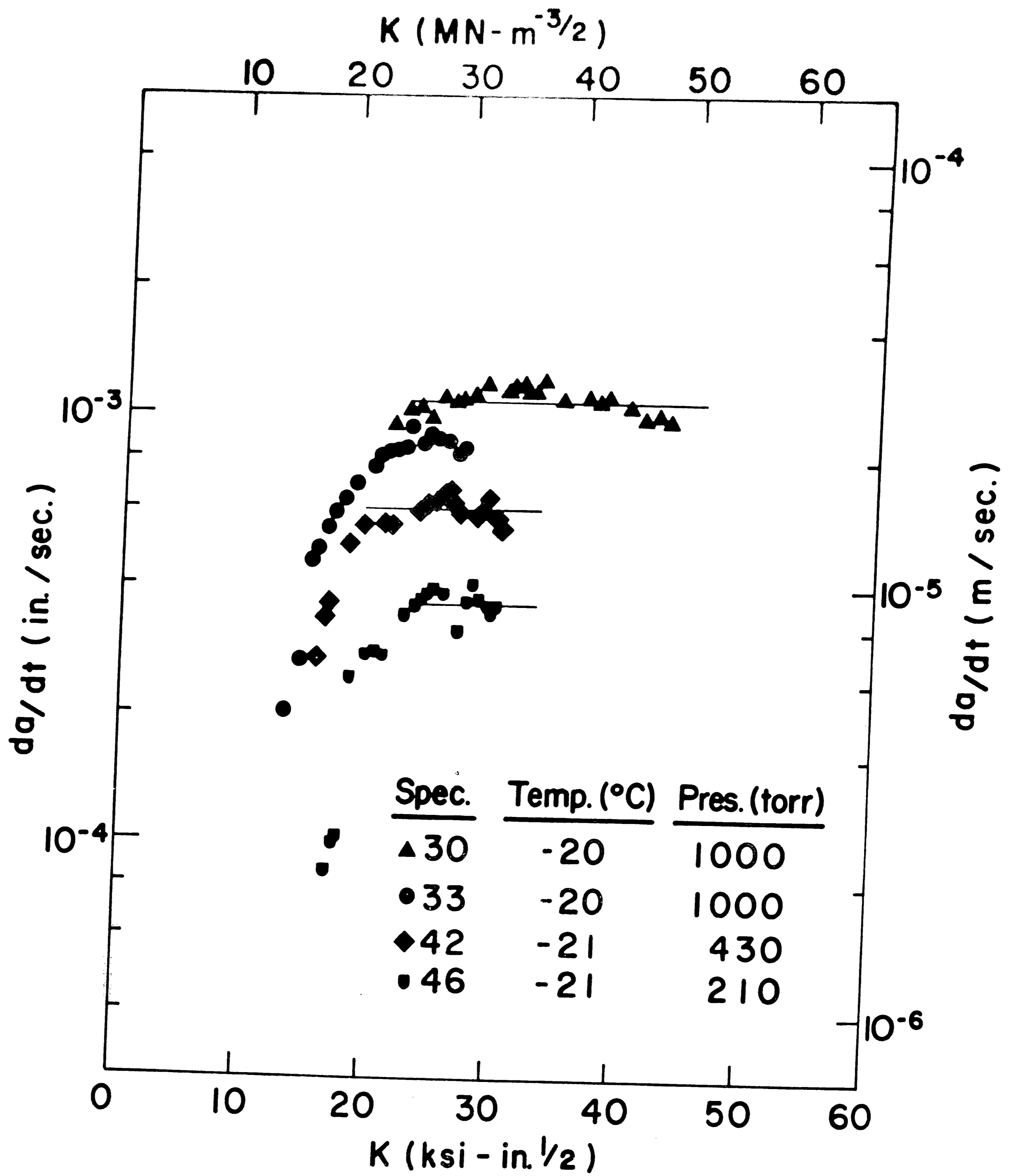


Figure 8: Hydrogen Enhanced Crack Growth at -20°C for Various Hydrogen Partial Pressures

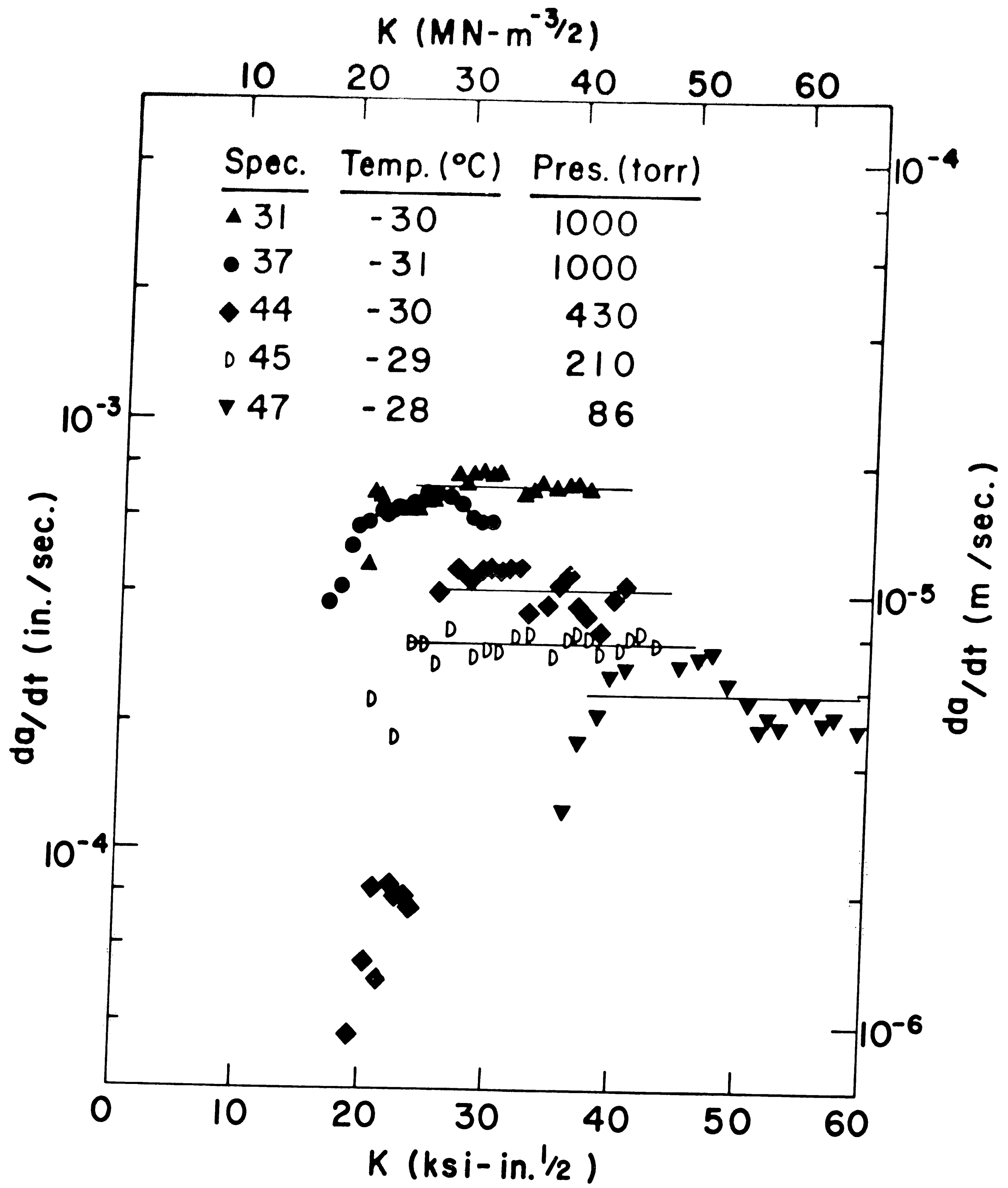


Figure 9: Hydrogen Enhanced Crack Growth at -30°C for Various Hydrogen Partial Pressures

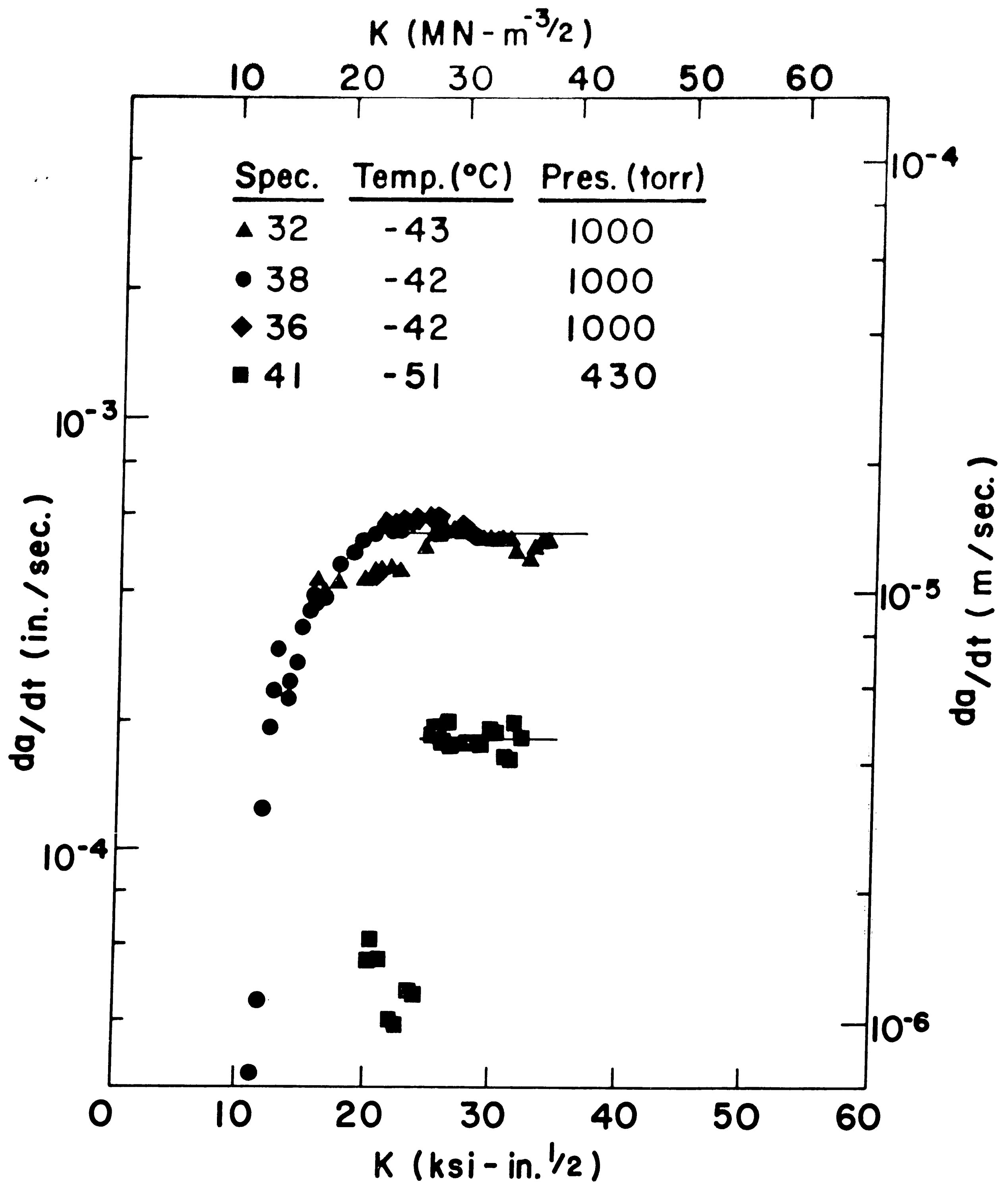


Figure 10: Hydrogen Enhanced Crack Growth at -42°C and -51°C

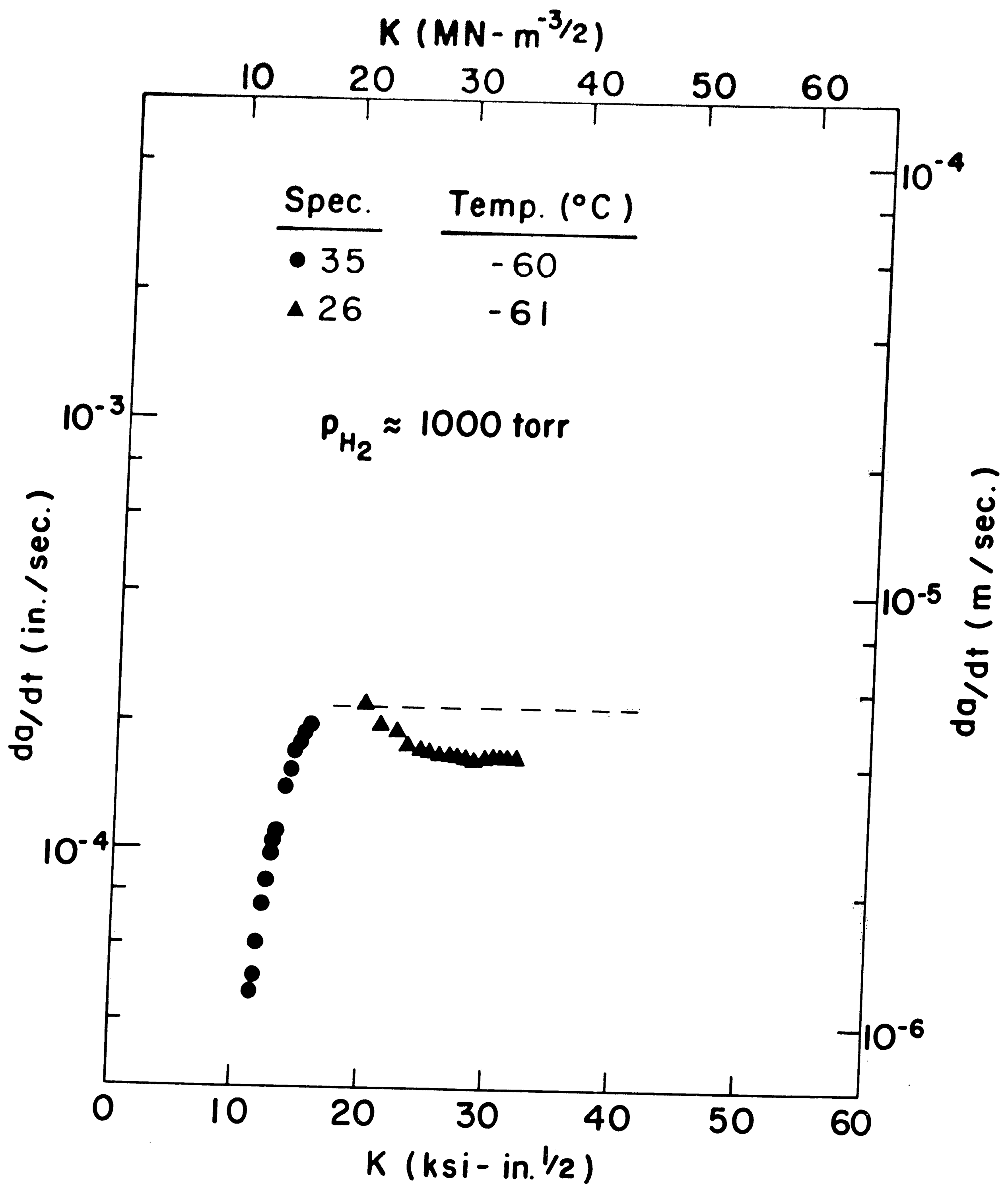


Figure 11: Hydrogen Enhanced Crack Growth at -60° C

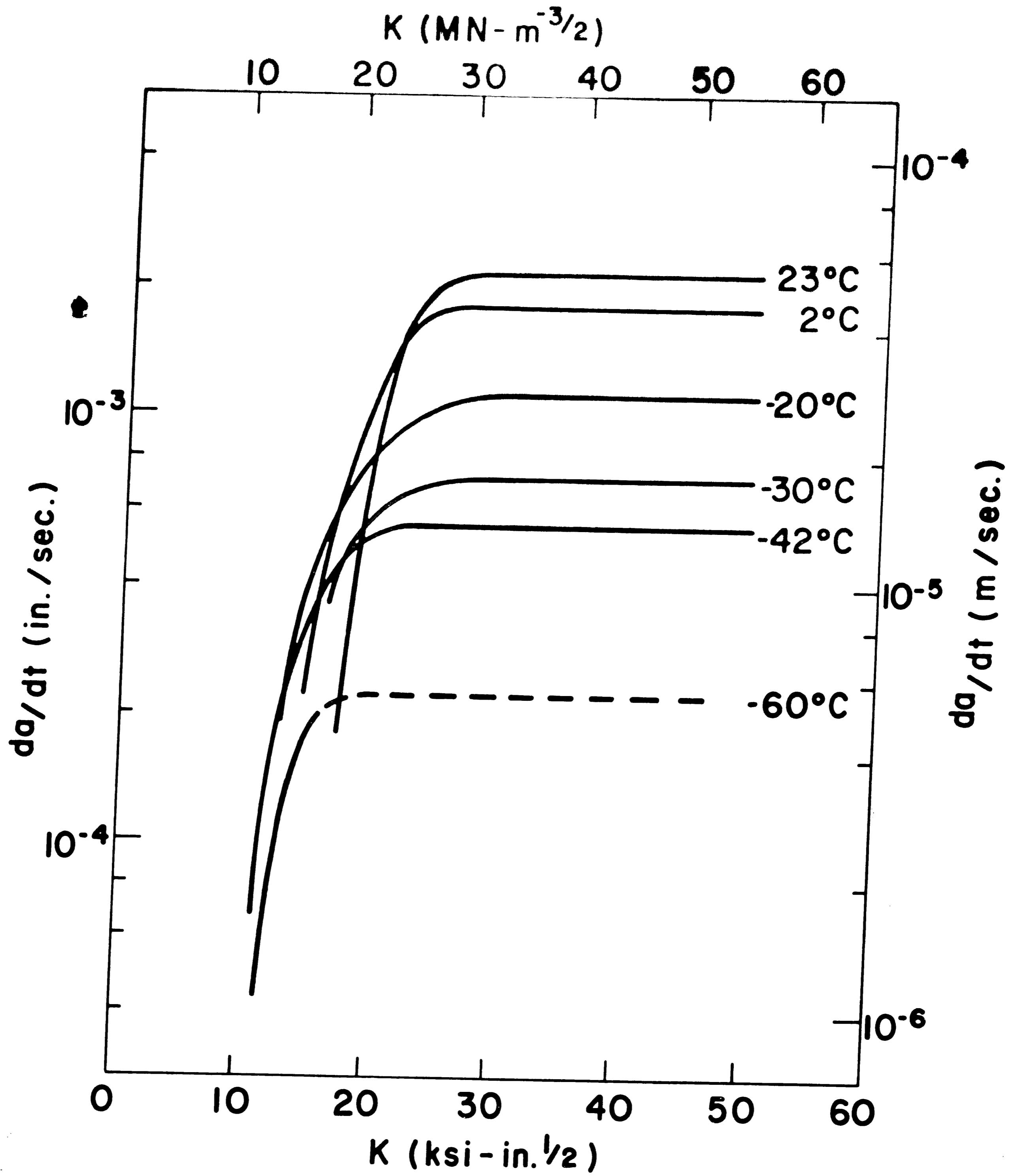


Figure 12: Composite of Hydrogen Enhanced Crack Growth Curves from 23°C to -60°C at a Hydrogen Pressure of ~1000 torr

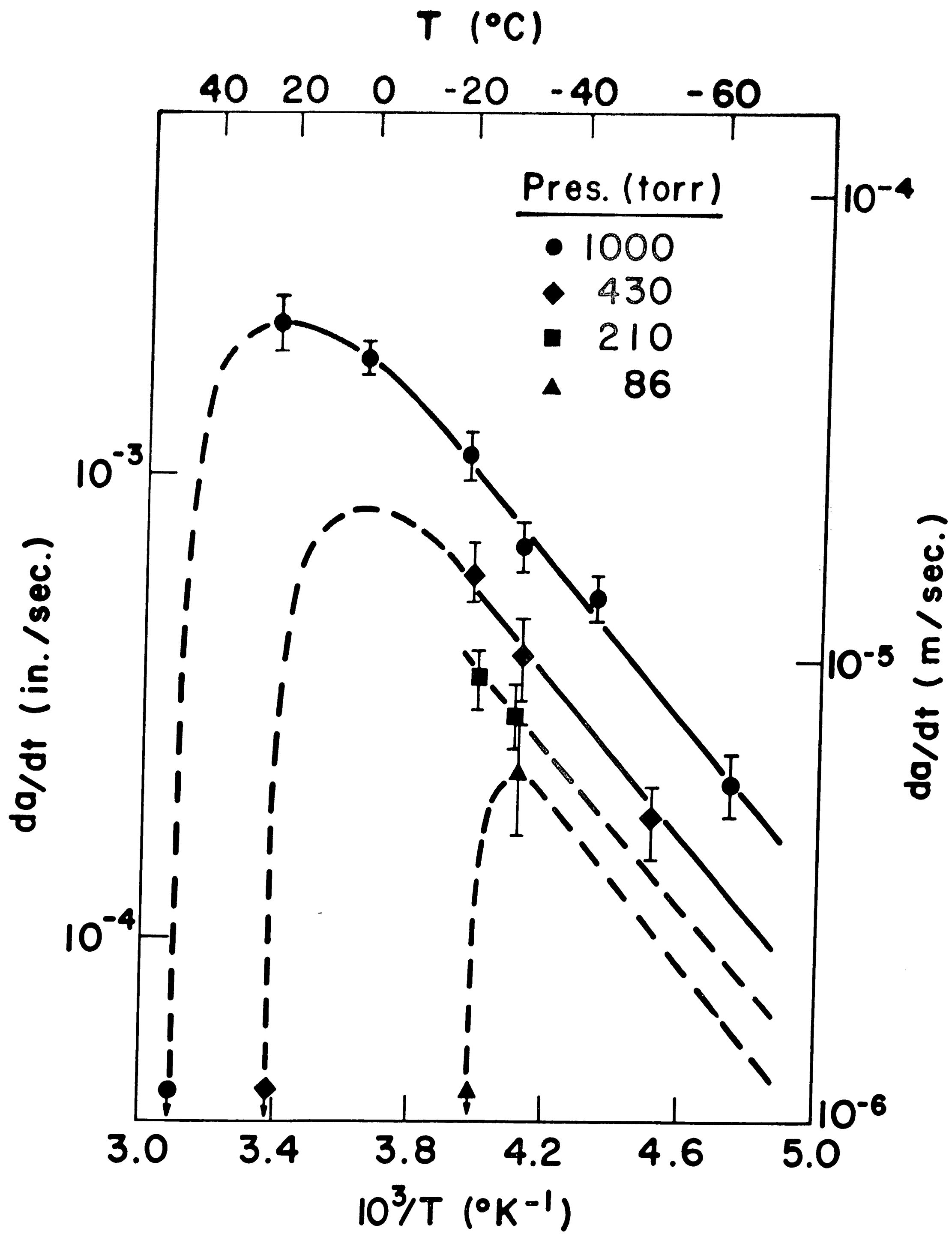


Figure 13: Effect of Temperature on Stage II Crack Growth for Various Hydrogen Partial Pressures

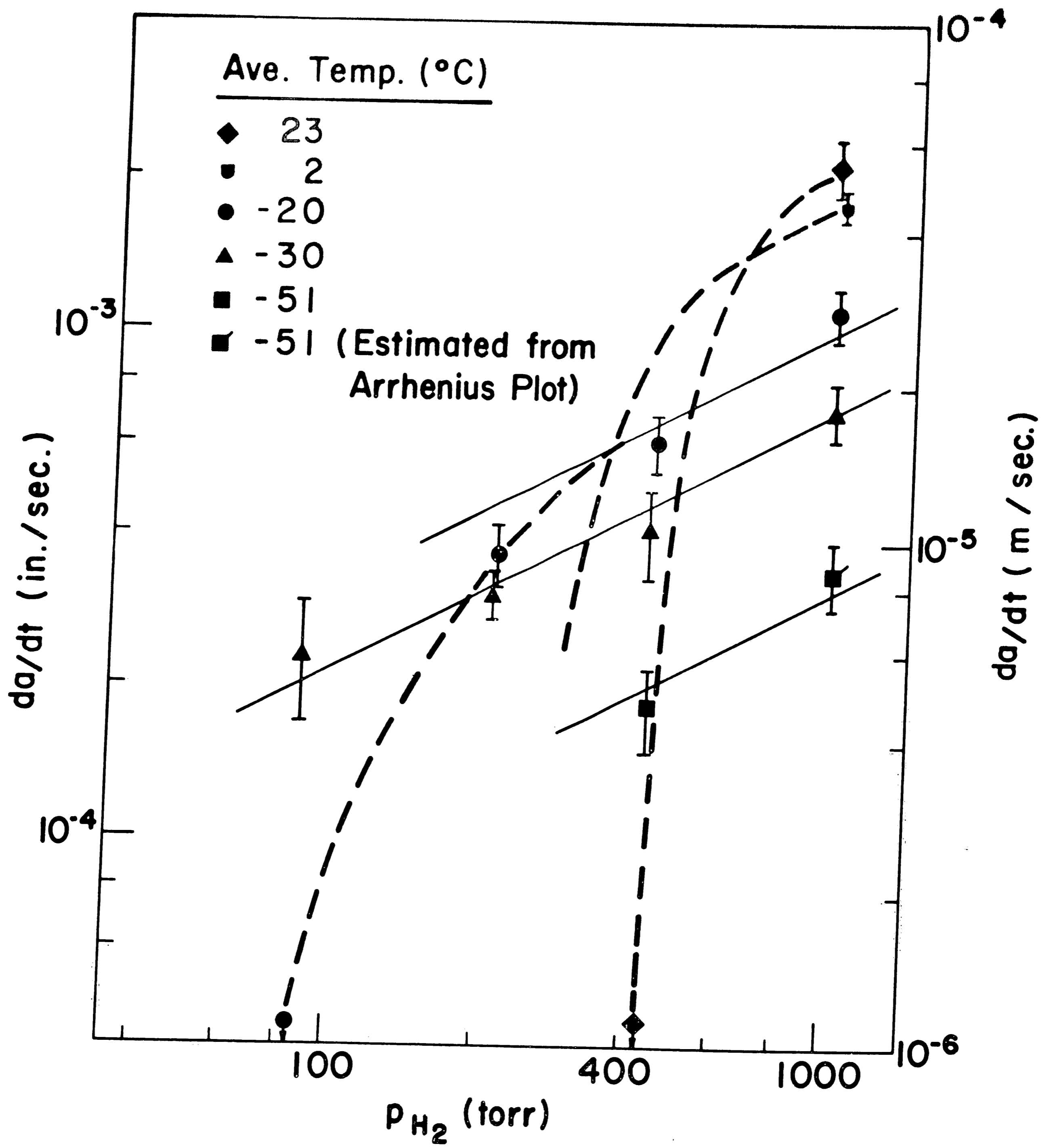


Figure 14: Effect of Hydrogen Partial Pressure on Stage II Crack Growth at Various Temperatures

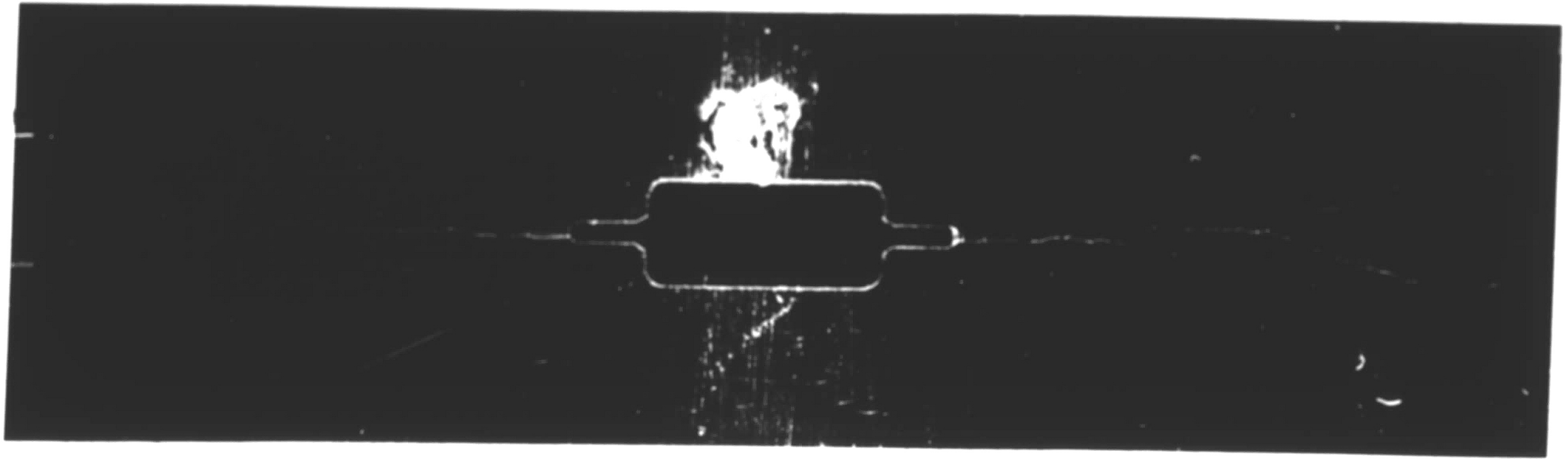


Figure 15: View of Severely Branched Crack at
1000 torr and -64°C , Side A

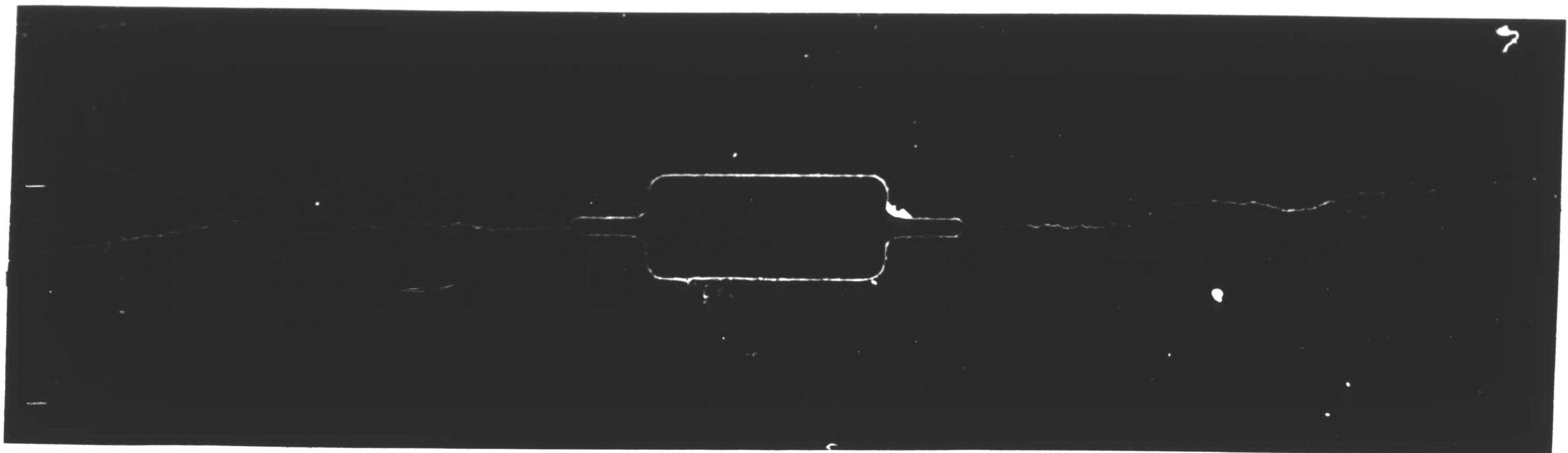


Figure 16: View of Severely Branched Crack at
1000 torr and -64°C , Side B

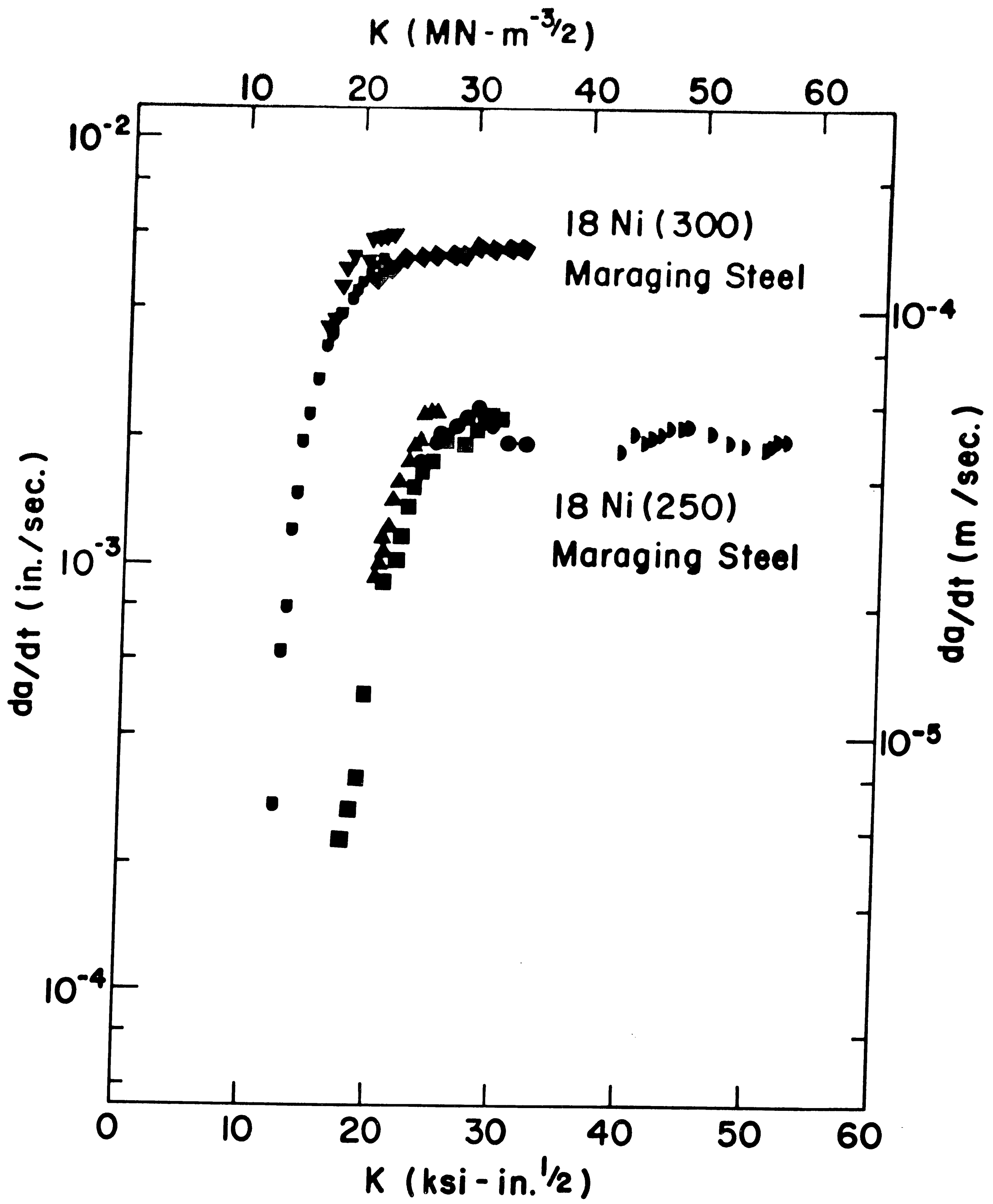


Figure 17: Effect of Strength Level on Hydrogen Enhanced Crack Growth in 18Nickel Maraging Steel

REFERENCES

1. J. H. Andres, A. K. Bose, H. Lee, and A. G. Quarrell, *Journal of the Iron and Steel Institute*, 146 (1942) 203.
2. J. H. Andres, H. Lee, A. K. Millik, and A. G. Quarrell, *Journal of the Iron and Steel Institute*, 153 (1946) 67.
3. C. R. Tottle and H. C. Wright, *The Metallurgy of Welding, Brazing and Soldering*, American Elsevier, New York (1960) 56.
4. H. J. Read, editor, *Hydrogen Embrittlement in Metal Finishing*, Reinhold, New York (1961).
5. C. A. Zappffe and N. E. Haslem, *Transactions of the American Society for Metals*, 39 (1947) 241.
6. R. H. Raring and J. A. Renbolt, *Transactions of the American Society for Metals*, 48 (1956) 198.
7. E. P. Klier, B. B. Muvdi and G. Sachs, *Proceedings of the American Society for Testing and Materials*, 58 (1958) 597.
8. R. M. Burns and W. W. Bradley, *Protective Coatings for Metals*, Reinhold, New York (1967).
9. L. S. Darken and R. P. Smith, *Corrosion*, 5 (1949) 1.
10. T. Broom and A. J. Nickolson, *Journal of Institute of Metals*, 89 (1960) 183.
11. A. S. Tetelman, *Proceedings of Conference - Fundamental Aspects of Stress Corrosion Cracking*, National Association of Corrosion Engineers, Houston (1969) 446.
12. S. M. Wiederhorn, *International Journal of Fracture Mechanics*, 42 (1968) 171.
13. H. C. Van Ness and B. F. Dodge, *Chemical Engineering Progress*, 51 (1955) 266.
14. D. D. Perlmutter and B. F. Dodge, *Industrial and Engineering Chemistry*, 48 (1956) 885.

15. W. Hofmann and W. Rauls, *Welding Journal*, 44 (1965) 225s.
16. R. A. Cavett and H. C. Van Ness, *Welding Journal*, 42 (1963) 3165.
17. J. B. Steinman, H. C. Van Ness and G. S. Ansell, *Welding Journal*, 44 (1965) 221s.
18. R. M. Vennett and G. S. Ansell, *Transactions Quarterly, ASM*, 62 (1969) 1007.
19. G. G. Hancock and H. H. Johnson, *AIME Transactions*, 236 (1966) 513.
20. D. P. Williams, *Scripta Metallurgica*, 2 (1968) 385.
21. R. J. Walter, R. P. Jewett and W. T. Chandler, *Material Science and Engineering*, 5 (1969) 98.
22. D. P. Williams and H. G. Nelson, *Metallurgical Transactions*, 1 (1970) 63.
23. R. P. Wei and J. D. Landes, *Materials Research and Standards*, 9, 7 (1969) 25.
24. J. D. Landes, Ph.D. Dissertation, Lehigh University (1970).
25. H. G. Nelson, D. P. Williams and A. S. Tetelman, *Metallurgical Transactions*, 2 (1971) 953.
26. I. M. Bernstein, *Material Science and Engineering*, 6 (1970) 9.
27. V. R. Sawicki, Ph.D. Dissertation, Cornell University (1971).
28. D. P. Williams, "A New Criterion for Failure of Materials by Environment-Induced Cracking," to be published 1972.
29. G. E. Kerns and R. W. Staehle, "Slow Crack Growth in Hydrogen and Hydrogen Sulfide Gas Environments," to be published 1972.
30. R. P. Wei, *Proceedings of Conference-Fundamental Aspects of Stress Corrosion Cracking*, National Association of Corrosion Engineers, Houston (1969) 104.
31. H. H. Johnson and P. C. Paris, *Journal of Engineering Fracture Mechanics*, 1, 1(1968) 3.

32. R. J. Bucci and P. C. Paris, *Corrosion*, 27, 12 (1971) 525
33. P. W. Bridgman, *Proceedings of the American Academy of Arts and Sciences*, 59 (1924) 173.
34. T. C. Poulter, *Transactions, ASME, Journal of Applied Mechanics*, 64 (1942) A31.
35. B. F. Dodge, *Transactions, ASME*, 75 (1953) 331.
36. R. L. Mills and F. J. Eduskuty, *Chemical Engineering Progress*, 52, 11 (1956) 477.
37. H. H. Johnson, J. G. Morlet and A. R. Troiano, *Transactions, AIME*, 212 (1958) 528.
38. E. A. Steigerwals, R. W. Schaller and A. R. Troiano, *Transactions, AIME*, 215 (1959) 1048.
39. R. A. Oriani, *Proceedings of Conference - Fundamental Aspects of Stress Corrosion Cracking, National Association of Corrosion Engineers, Houston, Texas* (1969).
40. D. O. Hayward and B. M. W. Trapnell, *Chemisorption, 2nd ed., Butterworths, Washington* (1964).
41. J. T. Brown and W. M. Baldwin, *Transactions, AIME*, 200 (1954) 298.
42. W. Beck, J. O'M. Bockris, J. McBreen and L. Nanis, *Proceedings of the Royal Society, London*, A290 (1966) 220.
43. A. S. Porter and F. C. Tompkins, *Proceedings of the Royal Society, London*, A217 (1953) 529.
44. R. A. Oriani, *Metallurgical Transactions*, 1 (1970) 2346.
45. W. F. Brown, Jr. and J. E. Srawley, *ASTM STP 410* (1966).
46. Isida, "Crack Tip Stress Intensity Factors for the Tension of an Eccentrically Cracked Strip," *Lehigh University, Dept. of Mech. Rep.* (1965).
47. J. E. Srawley and W. F. Brown, Jr., *ASTM STP 381* (1965) 133.

48. H. H. Johnson, *Materials Research and Standards*, 5 (1965) 422.
49. C. Y. Li and R. P. Wei, "Calibrating the Electrical Potential Method for Studying Slow Crack Growth," *Materials Research and Standards*, 6, 8 (1966) 392.
50. C. Zapffe and C. Sims, *AIME Transactions*, 145 (1941) 225.
51. F. deKazinczy, *Journal of the Iron and Steel Institute*, 177 (1954) 85.
52. F. Garofalo, Y. T. Chou and V. Ambegaokar, *Acta Metallurgica*, 8 (1960) 504.
53. B. A. Bilby and J. Hewitt, *Acta Metallurgica*, 10 (1962) 587.
54. A. S. Tetelman, W. D. Robertson, *Transactions AIME*, 224 (1962) 775.
55. N. J. Petch and P. Stables, *Nature*, 169 (1952) 842.
56. N. J. Petch, *Philosophical Magazine*, 1 (1956) 331.
57. R. P. Frohberg, W. J. Barnett and A. R. Troiano, *Transactions, ASM*, 47 (1955) 892.
58. A. R. Troiano, *Transactions ASM*, 52 (1960) 54.
59. S. J. Hudak and R. P. Wei, unpublished results (1971).
60. R. P. Wei, S. R. Novak and D. P. Williams, Paper No. 5, AGARD (NATO) Conference Proc. No. 98 (1971), and *Materials Research and Standards* 12, 9 (1972) 25.
61. S. M. Toy and A. Phillips, *Corrosion* 26, 7 (1970) 200.

VITA

The author, Stephen J. Hudak, Jr., son of Stephen J. and Loretta M. Hudak, Sr., was born in Bethlehem, Pennsylvania on June 11, 1948. He attended primary and secondary schools in Hellertown, Pennsylvania, and graduated from Saucon Valley High School in June 1966. He entered The Pennsylvania State University in September 1966 and received a Bachelor of Science degree in engineering mechanics in June 1970.

In July 1970 he began graduate study at Lehigh University in pursuit of the degree of Master of Science in Metallurgy and Materials Science. While there, he served as a research assistant with the Center for Surface and Coatings Research. In August 1972, he joined the Westinghouse Electric Corporation at the Research and Development Center in Pittsburgh, Pennsylvania.

He has been engaged in research in the area of environment sensitive mechanical behavior in high strength alloys. He has co-authored two publications: "The Influence of Loading Variables on Environment Enhanced Fatigue Crack Growth in High Strength Steels," to be published in ASTM's Journal of Materials, and a discussion of the paper "Effects of Cyclic Stress Form on Corrosion Fatigue Crack Propagation below K_{ISCC} in High-Yield-Strength Steel," by J. M. Barsom, in Proceedings of the International Conference on Corrosion Fatigue, Storrs, Connecticut, June 1971.

He married the former Jane Anne Deibert in June 1971.